Copy 6

RM A56H30

RESEARCH MEMORANDUM

AN ANALOG COMPUTER STUDY OF SEVERAL STABILITY AUGMENTATION SCHEMES DESIGNED TO ALLEVIATE ROLL-INDUCED INSTABILITY

By Brent Y. Creer

Ames Aeronautical Laboratory
Moffett Field, Calif.

NATIONAL ADVISORY COMMITTEE
FOR AERONAUTICS

WASHINGTON

February 19, 1957

NATIONAL ADVISORY COMMITTEE FOR AERONAUTICS

RESEARCH MEMORANDUM

AN ANALOG COMPUTER STUDY OF SEVERAL STABILITY AUGMENTATION SCHEMES DESIGNED TO ALLEVIATE ROLL-INDUCED INSTABILITY

By Brent Y. Creer

SUMMARY

An analog computer study has been made of several stability augmentation schemes designed to reduce the objectionable inertia coupling effects encountered in rolling maneuvers with the F-100A airplane having the original small vertical tail. These augmenters essentially limited the roll rate to below the critical value (approximately equal to the yawing or pitching frequency of the nonrolling airplane) or extended the critical roll rate, and were a roll-rate limiter, a sideslip limiter, an augmenter employing feedback proportional to the product of rolling velocity and pitching velocity to remove an inertia cross-coupling yawing moment, and combinations of the roll-rate limiter with each of the other two.

The results of this study showed that stability augmenters using single feedback quantities reduced the maximum angle of attack and sideslip excursions experienced during a roll maneuver to reasonable levels, but the required servo-control-surface deflection was so large as to make their use on the example airplane impractical, provided the original conventional control surfaces were used. However, with either combination of augmenter tested, this objection was alleviated but not entirely eliminated.

The effect of changes in the initial trim normal load factor was small, except when the angle of attack of the principal axis was large and the critical rolling velocity was exceeded. Changes in the flight-test speed and altitude generally required changing the feedback characteristics of all the augmentation systems, except for the sideslip limiter, where it appears as though a single set of servo feedback characteristics would suffice for all the speed and altitude conditions tested.

INTRODUCTION

Some current fighter aircraft have experienced violent pitching and yawing motions during aileron-induced roll maneuvers (refs. 1 and 2). The possibility of this occurrence was predicted by Phillips in reference 3, wherein he shows that, depending upon the amount of damping present in the longitudinal or directional oscillatory mode, a divergent yawing and pitching motion can occur during a steady roll when the rolling frequency exceeds a critical value, p_c, equal to the lower of the pitching and yawing natural frequencies of the nonrolling airplane. Thus two ways to reduce the objectionable yawing and pitching motions accompanying rolling maneuvers are: (1) limiting the rolling velocity below p_c of the basic airplane and (2) increasing the value of the critical rolling velocity by altering the stability characteristics of the airplane. The purpose of the present study is to investigate these suggested methods for reducing the undesirable pitching and yawing motions of an airplane during roll maneuvers. These methods were investigated using an electronic analog computer wherein changes in the airplane stability characteristics and roll-rate limiting were obtained by appropriate servo actuation of the control surfaces. The airplane characteristics used in this study were those of the F-100A airplane having the original small vertical tail as shown in figure 1.

NOTATION

B.P.	break point, radians per second in the case of the roll-rate limiter and degrees in the case of the sideslip limiter (See fig. 3.)
b	wing span, ft
$\bar{c}$	wing mean aerodynamic chord, ft
C_l	rolling-moment coefficient, $\frac{\text{rolling moment}}{qSb}$
C_{l_β}	$\frac{\partial C_l}{\partial \beta}$, per radian
C_{l_p}	$\frac{\partial C_l}{\partial (pb/2V)}$, per radian
C_{l_r}	$\frac{\partial C_l}{\partial (rb/2V)}$, per radian
$C_{l_{\delta_a}}$	$\frac{\partial C_l}{\partial \delta_a}$, per radian

[redacted]

C_m pitching-moment coefficient, $\frac{\text{pitching moment}}{qS\bar{c}}$

C_{m_α} $\frac{\partial C_m}{\partial \alpha}$, per radian

$C_{m_{\dot{\alpha}}}$ $\frac{\partial C_m}{\partial(\dot{\alpha}\bar{c}/2V)}$, per radian

C_{m_q} $\frac{\partial C_m}{\partial(q\bar{c}/2V)}$, per radian

$C_{m_{i_t}}$ $\frac{\partial C_m}{\partial i_t}$, per radian

C_N normal-force coefficient, $\frac{\text{normal force}}{qS}$

C_{N_α} $\frac{\partial C_N}{\partial \alpha}$, per radian

C_n yawing-moment coefficient, $\frac{\text{yawing moment}}{qSb}$

C_{n_β} $\frac{\partial C_n}{\partial \beta}$, per radian

C_{n_p} $\frac{\partial C_n}{\partial(pb/2V)}$, per radian

C_{n_r} $\frac{\partial C_n}{\partial(rb/2V)}$, per radian

$C_{n_{\delta_r}}$ $\frac{\partial C_n}{\partial \delta_r}$, per radian

$C_{n_{\delta_a}}$ $\frac{\partial C_n}{\partial \delta_a}$, per radian

C_Y side-force coefficient, $\frac{\text{side force}}{qS}$

C_{Y_β} $\frac{\partial C_Y}{\partial \beta}$, per radian

C_{Y_p}	$\frac{\partial C_Y}{\partial(pb/2V)}$, per radian
C_{Y_r}	$\frac{\partial C_Y}{\partial(rb/2V)}$, per radian
g	acceleration due to gravity, ft/sec^2
H_e	angular momentum of engine rotor, slug-ft^2-radians/sec, positive for clockwise rotation
h_p	pressure altitude, ft
i_t	horizontal stabilizer deflection, radians, except as noted
i_{ts}	horizontal stabilizer servo deflection, radians, except as noted
I_X	moment of inertia of airplane about X axis, slug-ft^2
I_{XZ}	product of inertia of airplane referred to X and Z axes, slug-ft^2
I_Y	moment of inertia of airplane about Y axis, slug-ft^2
I_Z	moment of inertia of airplane about Z axis, slug-ft^2
M	Mach number
m	mass of airplane, $\frac{W}{g}$, slugs
n	load factor, g
p	rolling velocity, radians/sec
p_c	rolling velocity at which roll-coupling instability is encountered
p_{c_1}, p_{c_2}	natural frequencies of nonrolling airplane
p_1	difference between actual rolling velocity and rolling velocity at which break point is set and is defined only if $\lvert p \rvert > \lvert p_{BP} \rvert$
q	pitching velocity, radians/sec, or dynamic pressure, $\frac{1}{2}\rho V^2$, lb/ft^2
R.R.L.	roll-rate limiter
r	yawing velocity, radians/sec

S	wing area, ft^2
S.S.L.	sideslip limiter
t	time, sec
Δt	incremental time, sec
V	true airspeed, ft/sec
W	airplane weight, lb
X,Y,Z	body axes of airplane
α	angle of attack of airplane body axis, radians, except as noted
β	angle of sideslip, radians, except as noted
β_1	difference between actual sideslip and sideslip value at which the break point is set and is defined only if $\lvert\beta\rvert > \lvert\beta_{BP}\rvert$
$\Delta\alpha$, $\Delta\beta$	increments measured from an initial trim condition, deg
δ_a	total aileron deflection, radians, except as noted
δ_{as}	aileron servo deflection, radians, except as noted
δ_r	rudder deflection, radians, except as noted
δ_{rs}	rudder servo deflection, radians, except as noted
ψ,θ,ϕ	angles of yaw, pitch, and roll, respectively
$\Delta\phi$	incremental bank angle, deg
ρ	mass density of air, $slugs/ft^3$
$\lvert\Delta\alpha\rvert$	absolute magnitude of the quantity $\Delta\alpha$
$(\dot{})$	derivative with respect to time

Subscripts

BP	break point (See fig. 3.)
Y,Z	body axes of airplane

[redacted]

PRELIMINARY CONSIDERATIONS

Equations of Motion

The airplane equations of motion and Eulerian angles used in this investigation are listed below and are written with respect to body axes as defined in reference 4. The axis system, with the positive direction of forces, moments, and angles, as used in this investigation, is shown in figure 2. The assumption of constant velocity along the longitudinal axis and the simplifications made to the Eulerian angle equations were not considered to affect seriously the results obtained and were made because of limitations in the computer capacity. The equations as listed contain the usual inertia terms and, in addition, the gyroscopic moments due to the jet engine. These engine terms were included, since previous analog computer studies, as well as the analysis of reference 5, indicated these terms could have an appreciable influence on the airplane motions.

$$\dot{\beta} = \alpha p - r + \frac{g}{V} \sin \phi + \frac{qS}{mV} \left(C_{Y_\beta} \beta + \frac{b}{2V} C_{Y_r} r + \frac{b}{2V} C_{Y_p} p \right)$$

$$\dot{\alpha} = q - \beta p + \frac{g}{V} \cos \phi - \frac{qS}{mV} C_{N_\alpha} \alpha$$

$$\dot{p} = \frac{I_{XZ}}{I_X} (\dot{r} + pq) + \left(\frac{I_Y - I_Z}{I_X} \right) qr + \frac{qSb}{I_X} \left(C_{l_\beta} \beta + \frac{b}{2V} C_{l_p} p + C_{l_{\delta_a}} \delta_a + \frac{b}{2V} C_{l_r} r \right)$$

$$\dot{q} = \frac{I_{XZ}}{I_Y} (r^2 - p^2) + \left(\frac{I_Z - I_X}{I_Y} \right) pr - \frac{H_e r}{I_Y} + \frac{qS\bar{c}}{I_Y} \left(C_{m_\alpha} \alpha + C_{m_{i_t}} i_t + \frac{\bar{c}}{2V} C_{m_q} q + \frac{\bar{c}}{2V} C_{m_{\dot{\alpha}}} \dot{\alpha} \right)$$

$$\dot{r} = \frac{I_{XZ}}{I_Z} (\dot{p} - qr) + \left(\frac{I_X - I_Y}{I_Z} \right) pq + \frac{H_e q}{I_Z} + \frac{qSb}{I_Z} \left(C_{n_\beta} \beta + \frac{b}{2V} C_{n_r} r + C_{n_{\delta_r}} \delta_r + C_{n_{\delta_a}} \delta_a + \frac{b}{2V} C_{n_p} p \right)$$

$$\dot{\phi} = p$$

$$\dot{\theta} = q \cos \phi - r \sin \phi$$

$$\dot{\psi} = q \sin \phi + r \cos \phi$$

Details of Stability Augmentation Systems

The general approach to the problem of reducing the objectionable airplane motions encountered during a rolling maneuver was indicated in the Introduction. The specific augmentation schemes which resulted from the general approach and which were investigated in this report are noted as follows:

1. A roll-rate limiter (nonlinear C_{l_p}) to prevent the rolling frequency from attaining the critical value.

2. Reference 3 defines the critical frequency in terms of the yawing and pitching natural frequencies of the nonrolling airplane as

$$p_{c_1} = \sqrt{\frac{qSbC_{n_\beta}/I_Z}{(I_Y-I_X)/I_Z}}, \qquad p_{c_2} = \sqrt{\frac{-qS\bar{c}C_{m_\alpha}}{I_Y}}$$

In view of the above formulas, a sideslip limiter (nonlinear C_{n_β}) was investigated. This augmentation system produced, in a sense, an increase in the directional frequency of the nonrolling airplane, or from a different point of view, provided a greatly increased C_{n_β} past a certain value of β in order to limit sideslip excursions. The nonlinear C_{n_β} variation was considered with the thought that it might be desirable to retain the normal directional stability and associated handling qualities around zero β.

3. Inspection of the equation for p_{c_1} shows that an additional way of increasing the yaw natural frequency would be to decrease the inertia term $(I_Y - I_X)/I_Z$. From the airplane yawing-moment equation it can be seen that by using a rudder servo system with feedback proportional to pq such as to null the inertia coupling term $[(I_Y - I_X)/I_Z]pq$, an effective increase in p_{c_1}, in a sense, can be accomplished. This stability augmentation system was termed a "pq device." A more detailed analysis defines p_{c_2} more precisely as

$$p_{c_2} = \sqrt{\frac{-qScC_{m_\alpha}/I_Y}{(I_Z - I_X)/I_Y}}$$

Hence another possible method would be to reduce the inertia coupling term $[(I_Z - I_X)/I_Y]pr$ in the pitching-moment equation.

4. Combinations of method 1 above with methods 2 and 3.

A simplified block diagram showing the basic components of the rudder, horizontal stabilizer, and aileron stability augmentation systems and the tie-in with the airplane dynamics is illustrated in figure 3. The dynamics of the servo systems were held constant for this investigation and were each represented by a second-order system with a natural frequency of 5 cycles per second and a damping ratio of 0.40. The general form of the roll-rate limiter and sideslip limiter feedback characteristics is shown in figure 3, from which can be seen the definition of roll-rate limiter and sideslip limiter break point. For this investigation, the transfer function of the sensing devices which would be used to measure p, q, β, etc., was taken as unity.

Estimation of Aerodynamic Derivatives

The first estimates of the linear aerodynamic derivatives used in this investigation were obtained from references 6 through 9 and from unpublished data obtained from NACA High-Speed Flight Station. Certain additional refinements were made to the values of the aerodynamic derivatives for those speed and altitude conditions where flight time histories were available of the response of the F-100A airplane to elevator or rudder pulses. These changes to the derivatives were made using the "cut-and-try" technique wherein the pilot-applied control-surface deflections were used as inputs to the computer and the values of the derivatives were adjusted until the computed airplane response and flight time history were in satisfactory agreement. Figures 4(a) and 4(b) show comparisons of the flight time histories of the airplane with the analog result for a rudder pulse at $M = 0.71$, $h_p = 30{,}700$ and $M = 0.90$, $h_p = 40{,}000$, respectively. Figure 4(c) shows similar results for a stabilizer pulse at $M = 0.9$, $h_p = 40{,}000$.

It should be pointed out that these flight time histories fit into the small perturbation category and were fitted adequately by using linear stability derivatives. However, in order to match the motions when the α and β excursions are large, as in a rolling maneuver where inertial coupling divergence is encountered, it is necessary to introduce certain

nonlinear stability derivatives. Figure 5 compares the extreme flight maneuver of figure 7, reference 1, with the analog computed response using C_{l_β} and C_{n_β} nonlinearities of a form suggested in reference 8 and shown in figure 6. The approximation to the actual aerodynamic derivatives, as evidenced by the match between the flight and computed response, was taken to be sufficient for the purposes of this investigation. It was surmized that the general form of the nonlinearities would hold for the remaining test speed and altitude conditions; however, the slope of the C_{l_β} versus angle-of-attack curve and the base value of the C_{n_β} curve (fig. 6) were modified to take account of Mach number effects. The complete set of aerodynamic derivatives and mass parameters used in this investigation is shown in the aforementioned figure and table I.

Method of Analysis

The airplane-servo combination was evaluated on the basis of its response characteristics in an aileron-induced roll. Responses were obtained for a range of aileron deflections up to 30° for a basic input which consisted of a ramp of 50° per second to the desired deflection followed by a return to neutral when the airplane had rolled to a specified bank angle. The pilot's rudder and elevator were held constant during this maneuver. The input aileron deflections were in a direction to cause negative rolling rates, since the α and β excursions, for the example configuration studied, were generally larger in left rolls. Figure 7 shows a typical computed record on which has been labeled the quantities used in plotting the results of this investigation.

The specified bank angle through which the airplane was rolled and the trim normal load factors from which the roll maneuvers were initiated for the speed and altitude conditions at which each stability augmentation scheme was tested are shown in the following table:

Speed and altitude	$\Delta\phi$, deg	Roll-rate limiter	Sideslip limiter	pq device	pr device	Combination roll-rate and sideslip limiter	Combination roll-rate limiter and pq device
M = 0.7, h_p = 32,000	360	1g, -1g, 2g	1g, -1g, 2g	1g, -1g, 2g	1g	1g, -1g, 2g	1g, -1g, 2g
M = 0.9, h_p = 40,000	360	↓	↓	↓	---	---	---
M = 1.3, h_p = 40,000	720	↓	↓	↓	---	1g, -1g, 2g	1g, -1g, 2g
M = 0.9, h_p = 5,000	720	↓	↓	↓	---	---	---

[redacted]

The bank angle of 720° was used for the high dynamic-pressure flight conditions in order to allow a larger build-up in the α and β excursions, hence providing a better basis on which to compare the various stability augmentation schemes.

RESULTS AND DISCUSSION

The following discussion of the effect of the various feedback quantities used in each augmentation system on the airplane's rolling response applies, generally, to all flight conditions tested. However, the results presented in figures 8 through 23 are specifically for the case $M = 0.7$, $h_p = 32{,}000$ with an initial normal acceleration of 1g. The results for this speed and altitude were presented not only because they were qualitatively typical but also because the unaugmented airplane was unstable, in the inertia coupling sense, through a rather large range of aileron deflections; hence any failing or weakness of an augmentation scheme was accentuated. For the same reason, the results presented in figures 24 through 26, which show the effect of initiating the roll maneuver from different trim normal load factors, are also taken from the $M = 0.7$, $h_p = 32{,}000$ flight condition. The final part of the discussion is concerned with the effect of speed and altitude changes on the rolling response and associated system feedback characteristics and the supporting results are presented in figures 24, 27, 28, and 29. The data in these figures are for an initial normal load factor of 1, rather than load factors of -1 or 2, because the α, β, and servo-control-surface deflections for this case were generally larger. The single notable exception was the $M = 0.7$, $h_p = 32{,}000$ case.

Roll-Rate Limiter

The effect of roll-rate limiter gearing and break point on the airplane motions during an aileron-induced roll maneuver is illustrated in figures 8 and 9, respectively, for input aileron deflections between 6° and 30°. A cross plot at $\delta_a = 30°$ of the data such as that contained in these two figures is shown in figure 10. It can be seen from this figure that for a given gearing, there is a well-defined best break point, in the sense that α and β excursions are maintained to relatively small values and the required servo deflection is a minimum. As the break point is increased beyond this best value, α, β, and δ_{as} increase rapidly, with the airplane motion finally going divergent for break-point values in the neighborhood of p_c, the critical rolling velocity. This apparent instability is characterized by the airplane continuing to roll with nearly constant rolling velocity and the α and β excursions increasing with time, even after the aileron input has been neutralized. The area of this

[redacted]

divergence is noted on the figures by a cross-hatch boundary. The most notable effect of increasing the gearings is to cause a corresponding increase in the best break-point value, hence allowing larger maximum roll rates.

It should be pointed out that the required aileron servo deflection varies with both break point and gearing, with a minimum value of approximately 20° being required for the subject case. This relatively large value of aileron deflection was required because the minimum aileron input of 13° required to produce p_c was so small compared to the available 30° input deflection for which roll-rate limiting must be provided.

In conclusion, it can be seen that for the given flight condition a roll-rate limiter break point and gearing could be determined which would maintain the α and β excursions experienced during a roll maneuver to a reasonable level. The main drawback of this device is that the rolling performance may be so severely limited as to make the airplane unsuitable for its intended combat mission.

Sideslip Limiter

The effect of sideslip limiter feedback variables, namely break point and gearing, on the angular excursions in α and β and on the required rudder servo deflection is shown in figures 11, 12, and 13. The variation in the angle of attack and sideslip excursions with changes in the feedback variables was as expected, in that decreasing the break point and/or increasing the gearing generally reduces the α and β displacements. The variation of rudder servo deflection with gearing and break point depended to a limited extent on the flight condition and, hence, figures 11 through 13 are not completely typical. However, from a gross point of view, the required rudder servo deflection generally increased with larger feedback gearings. The variation with break point was somewhat inconsistent, at least over the useful range of break-point values (less than 5°) and depended upon the magnitude of δ_a. Figure 13 is typical in this last respect.

From figures 11 through 13, it can be seen that a break point and gearing could be determined which would prevent roll divergence and would limit the α and β excursions to reasonable values for rolling velocities attainable with the ailerons fully deflected. With regard to choice of break point in an operational system, it should be noted that even though the zero break-point case resulted in the best rolling characteristics, break-point values as large as 5° still resulted in what appears to be satisfactory rolling motions; hence the choice of break point would probably resolve itself on the resulting handling qualities of the airplane. For the subject case, maximum rudder servo deflections of the order of 35° were necessary, indicating an all-moving vertical tail might be necessary in order to obtain the control-surface effectiveness required to realize the full benefits of this type of stability augmentation.

pq Device

Figures 14 and 15 show the effect of feedback gearing, δ_{rs}/pq, on the angular excursions in α and β, and on the required rudder servo deflections during the previously described rolling maneuver. It can be seen that there is an optimum gearing which served to limit α and β excursions to moderate values for aileron inputs up to the 30° maximum. However, for the range of gearings which would probably be used in an operational system, the required rudder servo deflection was around 35°. Hence, as in the sideslip limiter case, an all-moving vertical stabilizer would be necessary to realize the full benefits of this type of stability augmentation. In view of the large required control-surface deflection, a check was made to determine the effect of limiting the rudder servo deflection to ±20°. The results were quite favorable in that the α and β excursions were only 20 percent greater than in the corresponding case where servo deflections of 35° were used.

A cursory investigation was made to determine the effect of an augmentation system employing both pq and pr feedback. Use of pr feedback corresponds to cancellation of the coupling term $[(I_Z - I_X)/I_Y]pr$ in the airplane pitching-moment equation and was accomplished by servo actuation of the horizontal stabilizer. From figure 16 it can be seen that for the range of i_{ts}/pr gearings used ($i_{ts}/pr = +0.065$ just cancels the $[(I_Z - I_X)/I_Y]pr$ term for constant roll velocity, whereas $i_{ts}/pr = -0.065$ doubles the effect of this term) only small gains were made by the addition of this feedback quantity for this particular case. It should be pointed out that the angular excursions in α, β, and δ_{rs} were largest for the case where both inertia coupling terms were just canceled (i.e., $\delta_{rs}/pq = -0.54$, and $i_{ts}/pr = +0.065$). These results were unexpected in view of the previously outlined suppositions. Further investigation showed that these unexpected results were caused by the transient motion which followed when the input aileron deflection was neutralized, and that if the ailerons were held deflected, thereby allowing the airplane to roll continuously until steady-state conditions were attained, the relative magnitudes of the steady-state values of α, β, etc., for each of the subject cases, conformed with that which was expected.

A limited investigation of the above method of using pq and/or pr feedback to prevent rolling divergence was reported in reference 10.

Sideslip limiter and roll-rate limiter.- The combined effect of sideslip limiter and roll-rate limiter break point on α, β, δ_{as}, and δ_{rs} during a 360° rolling maneuver is shown in figures 17, 18, and 19. For this case, reducing sideslip-limiter break point caused some reduction in α, β, and δ_{rs}; however, the most favorable effect was the reduction of

$\delta_{as,max}$. It can be seen that reducing the sideslip-limiter break point from 5° to 0° resulted in an approximate 50-percent reduction in the required aileron servo deflection. Changing the roll-rate limiter break point produced results similar to those outlined for the sideslip limiter break-point case, except here the most favorable effect was in the reduction of $\delta_{rs,max}$. As can be seen from figures 18 and 19, reducing the roll-rate limiter break point from 2.0 to 1.0 radians per second caused an approximate 55-percent reduction in the required rudder servo deflection.

Roll-rate limiter and pq device.- A combination pq device and roll-rate limiter was investigated with results similar to those of the combination sideslip limiter and roll-rate limiter. As can be seen from figures 20 and 21, reducing the roll-rate limiter break point had some effect on the α and β excursions; however, there was a very marked reduction on the required rudder servo deflection, amounting to approximately 50-percent, in going from a roll-rate limiter break point of 2 radians per second to 1 radian per second. The most notable effect of changing the δ_{rs}/pq gearing, at least through that range of gearing which would probably be used in an operational system, was on the required rudder servo deflection, figures 22 and 23. From figure 22 it can be seen that going from a δ_{rs}/pq gearing of -0.90 to -0.54 caused a 50-percent reduction in $\delta_{rs,max}$.

Comparison of Various Augmentation Schemes

Standard test conditions.- A comparison of the various augmentation systems during aileron-induced roll maneuvers initiated from a +1g trim condition at $M = 0.7$, $h_p = 32,000$ is made in figure 24. The feedback characteristics for each augmentation scheme compared were selected such that the angular excursions in α and β were limited to reasonable values and at the same time the most economical use was made of the servo-control-surface deflection. It can be seen that the augmentation schemes employing pq feedback or sideslip feedback are generally comparable. The α and β excursions are maintained to fairly low values in each case and the required rudder servo deflection is nearly the same. In comparing these two systems with the other stability augmentation schemes, it can be seen that perhaps their biggest advantage is that they place no restriction on the rolling rates of the airplane; as was pointed out previously their principal disadvantage was the inordinate servo-control-surface deflection required. The roll-rate limiter compares favorably with the sideslip limiter or pq device in that feedback characteristics can be determined which will maintain the α and β excursions to a reasonable level. However, as was previously pointed out, aileron servo deflection is excessive and restrictions are placed on the rolling performance of the airplane. By the employment of feedback quantities in combination a compromise is reached between augmentation systems employing pq or β feedback and the

roll-rate limiter system. The roll-rate restrictions may be eased, as compared with the roll-rate limiter case, and the required rudder servo deflection can in some cases be reduced as much as 50 percent while the α and β excursions are still maintained to reasonable levels.

Effect of trim normal load.- The effect of initiating the rolling maneuver from a -1g wings-level trim condition and from a 2g coordinated-turn trim condition on the augmented airplane rolling response is illustrated in figures 25 and 26, respectively. For the flight conditions tested there were only minor effects on the angular excursions and servo-control-surface requirements when the roll was initiated from -1g as compared with the 1g case. In the case of the unaugmented airplane, initiating the aileron rolls from a 2g coordinated turn causes additional induced rolling moments which oppose those caused by the input aileron disturbance and, therefore, larger input aileron deflection is required to produce the critical rolling velocity. In addition, when the divergent region is entered the airplane motions are much more violent. The consequence of the foregoing was that, for most flight conditions tested, the available aileron deflection for the augmented airplane rolling from a 2g normal load was insufficient to attain the most critical roll velocity regions; hence, the angular excursions in α and β as well as the required servo deflection did not exceed those of the corresponding 1g cases. However, there were exceptions to this, notably the $M = 0.7$, $h_p = 32{,}000$ case. From figure 26, it can be seen that the augmenters employing pq or β feedback did not contain the motions as well as in the 1g case.

Other test conditions.- Summary plots for aileron rolls from a 1g wings-level trim condition, which compare the various augmentation schemes for the remaining speeds and altitudes tested, are shown in figures 27, 28, and 29. It can be seen that in all cases feedback characteristics could be determined which would maintain the transverse and normal accelerations to reasonable values. Most of the feedback characteristics varied with flight condition; however, this is not surprising in view of the fact that the critical rolling velocity also varies with speed and altitude. The pq feedback gearing used in each case was that which would just balance out the inertia term $pq[(I_Y - I_X)/I_Z]$, in the steady-state sense. Roll-rate limiter break point depended on p_c and the amount of aileron deflection in excess of that required to produce the critical rolling velocity. The average value at which the break point was set for the cases tested was approximately 70 percent of p_c. Some changes in the aileron servo gearing with flight condition were necessary in order to prevent a high-frequency, closed-loop instability associated with the airplane-aileron-servo combination. The approximate gearing at which this instability occurred was predicted using a simplified analysis wherein the airplane is reduced to a single-degree-of-freedom system in roll, and the roll-rate limiter is reduced to a linear gain change; that is, the break point is reduced to zero and the gearing for which the analysis is to be made is retained. Although some changes in the sideslip limiter gearing were made with changes in flight conditions, it appeared that a single gearing and

break-point value of -6.0° per degree and ±2.5°, respectively, would have been suitable for all flight conditions tested. Feedback characteristics for augmentation schemes employing feedback quantities in combination varied in a manner similar to the single feedback cases discussed above.

CONCLUDING REMARKS

An analog computer study of the effects of several stability augmentation schemes designed to reduce the objectionable yawing and pitching motions encountered in rolling maneuvers with the F-100A airplane having the original small vertical tail has been made. From the results of this investigation the following concluding remarks can be stated.

It was found that break-point and gearing values for the roll-rate limiter could be determined which would limit the angle-of-attack and sideslip excursions to reasonable values; however, to achieve this it was necessary to restrict the rolling velocity of the airplane to approximately 75 percent of the critical value. Break point varied with the critical rolling velocity, whereas some decrease in the aileron servo gearing was required for large increases in the dynamic pressure. Aileron servo deflection of approximately two-thirds of the total available aileron deflection was necessary in order to realize the full benefits of this type of stability augmenter.

The sideslip limiter reduced the magnitudes of angle of attack and sideslip to reasonable levels for aileron inputs up to the maximum available of 30°. In addition, it appeared as though a single value of break point and gearing could be used for all speed and altitude conditions tested. The disadvantage of this system was that the required rudder servo deflection was about 35° and could even be greater under certain flight conditions when the roll maneuver is initiated from a 2g normal load trim condition. Since the maximum available rudder deflection was ±20°, an all-moving vertical stabilizer would probably be necessary in this instance to realize the full benefits of this type of augmentation.

The results for an augmentation scheme using feedback to the rudder proportional to the product of rolling and pitching velocity, to cancel out an inertia coupling term ($pq[(I_Y - I_X)/I_Z]$) in the yawing-moment equation of motion, were very similar to those for the sideslip limiter. The only notable difference was that there was an optimum gearing which served to limit the angle-of-attack and sideslip excursions to moderate values. In this case the gearing varied with speed and altitude and was approximately that value which, for a constant rolling velocity, would just balance out the inertia coupling term.

The simultaneous use of a sideslip limiter and roll-rate limiter eased the roll-rate restrictions as compared to those of the roll-rate

limiter alone, and the required rudder servo deflection, at some flight conditions tested, were reduced as much as 50 percent compared to those of the sideslip limiter alone. Feedback characteristics for augmentation schemes employing combination feedback quantities varied with flight condition in a manner similar to the single feedback cases discussed above.

A combination roll-rate limiter and pq device (an augmentation scheme using feedback proportional to the product of rolling and pitching velocity) was also investigated, with results very similar to the sideslip limiter and roll-rate-limiter combination.

Ames Aeronautical Laboratory
National Advisory Committee for Aeronautics
Moffett Field, Calif., Aug. 30, 1956

REFERENCES

1. NACA High-Speed Flight Station: Flight Experience With Two High-Speed Airplanes Having Violent Lateral-Longitudinal Coupling in Aileron Rolls. NACA RM H55A13, 1955.

2. Wesesky, John L., and Stephens, Robert L.: Phase II Flight Tests of the YF-102A Airplane, USAF S/N 53-1787. TR-55-31, Air Force Flight Test Center, Edwards Air Force Base, Aug. 1955.

3. Phillips, William H.: Effect of Steady Rolling on Longitudinal and Directional Stability. NACA TN 1627, 1948.

4. Abzug, M. J.: Kinematics and Dynamics of Fully-Maneuvering Airplanes. Rep. ES-16144, Douglas Aircraft Co. Inc., El Segundo, June 15, 1955.

5. Gates, Ordway B., and Woodling, C. H.: A Theoretical Analysis of the Effect of Engine Angular Momentum on Longitudinal and Directional Stability in Steady Rolling Maneuvers. NACA RM L55G05, 1955.

6. Wolowicz, Chester H.: Time-Vector Determined Lateral Derivatives of a Swept-Wing Fighter-Type Airplane With Three Different Vertical Tails at Mach Numbers Between 0.70 and 1.48. NACA RM H56C20, 1956.

7. Drake, Hubert M., Finch, Thomas W., and Peele, James R.: Flight Measurements of Directional Stability to a Mach Number of 1.48 for an Airplane Tested With Three Different Vertical Tail Configurations. NACA RM H55G26, 1955.

[redacted]

8. Jaquet, Byron M., and Fletcher, H. S.: Wind-Tunnel Investigation at Low Speed of Sideslipping, Rolling, Yawing, and Pitching Characteristics for a Model of a 45° Swept-Wing Fighter-Type Airplane. NACA RM L55F21, 1955.

9. Runckel, Jack F., and Schmeer, James W.: The Aerodynamic Characteristics at Transonic Speeds of a Model With a 45° Sweptback Wing, Including the Effect of Leading-Edge Slats and a Low Horizontal Tail. NACA RM L53J08, 1954.

10. Phillips, William H.: Analysis of An Automatic Control to Prevent Rolling Divergence. NACA RM L56A04, 1956.

[redacted]

TABLE I.- STABILITY DERIVATIVES AND MASS PARAMETERS USED IN F-100 ROLL-COUPLING STUDY

[1]Stability derivatives (per radian)	M = 0.70 h_p = 32,000	M = 0.90 h_p = 40,000	M = 0.90 h_p = 5,000	M = 1.3 h_p = 40,000
C_{Y_β}	-0.62	-0.66	-0.66	-0.47
C_{Y_r}	.34	.34	.33	.33
C_{Y_p}	.15	.17	.19	.10
C_{l_β}	← See figure 5 →			
C_{l_p}	-.21	-.32	-.32	-.40
C_{l_r}	.09	.13	.12	-.004
$C_{l_{\delta_a}}$	-.044	-.056	-.056	-.037
C_{n_β} (basic)	.039	.06	.064	.048
C_{n_r}	-.26	-.40	-.40	-.30
C_{n_p}	-.034	-.031	-.038	-.026
$C_{n_{\delta_r}}$	-.032	-.039	-.039	-.009
$C_{n_{\delta_a}}$	0	0	0	-.003
C_{N_α}	4.29	4.66	4.67	3.32
C_{N_δ}	0	0	0	0
C_{m_α}	-.42	-.84	-.84	-.90
$C_{m_{i_t}}$	-1.0	-.90	-.90	-.60
C_{m_q}	-3.75	-6.0	-6.0	-4.13
$C_{m_{\dot{\alpha}}}$	-1.25	-2.0	-2.0	-1.38

[1]All derivatives are with respect to airplane body axes. Derivatives are referred to a nominal center-of-gravity position of 30-percent $\bar{c}$.

S = 377 ft^2 I_X = 10,976 slug-ft^2 I_{XZ} = 942.3 slug-ft^2
b = 36.6 ft I_Z = 64,975 slug-ft^2 m = 745 slugs
$\bar{c}$ = 11.3 ft I_Y = 57,100 slug-ft^2 H_e = 17,554 slug-ft^2-radians/sec

[redacted]

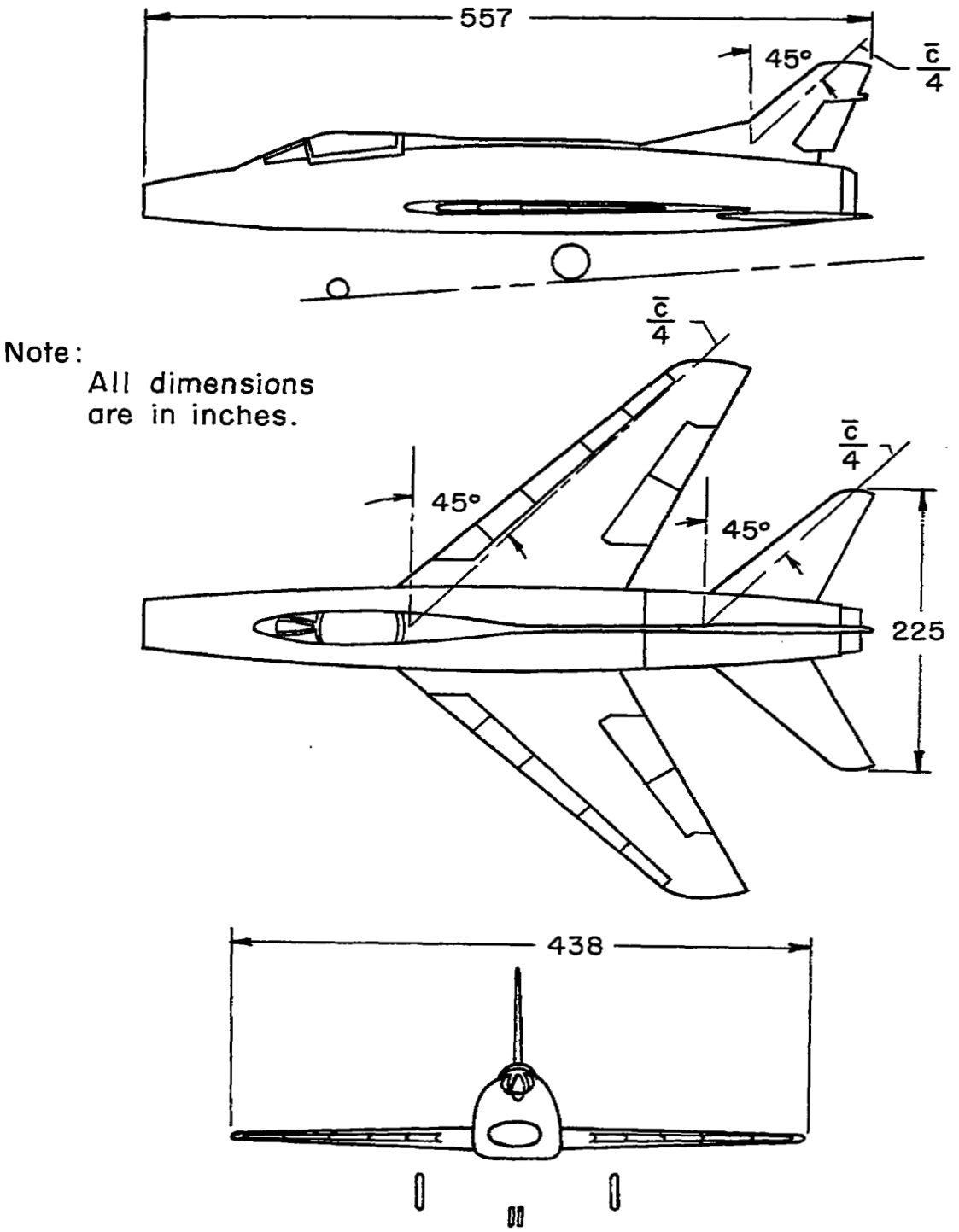

Figure 1.- Three-view drawing of F-100A with original small vertical tail.

[redacted]

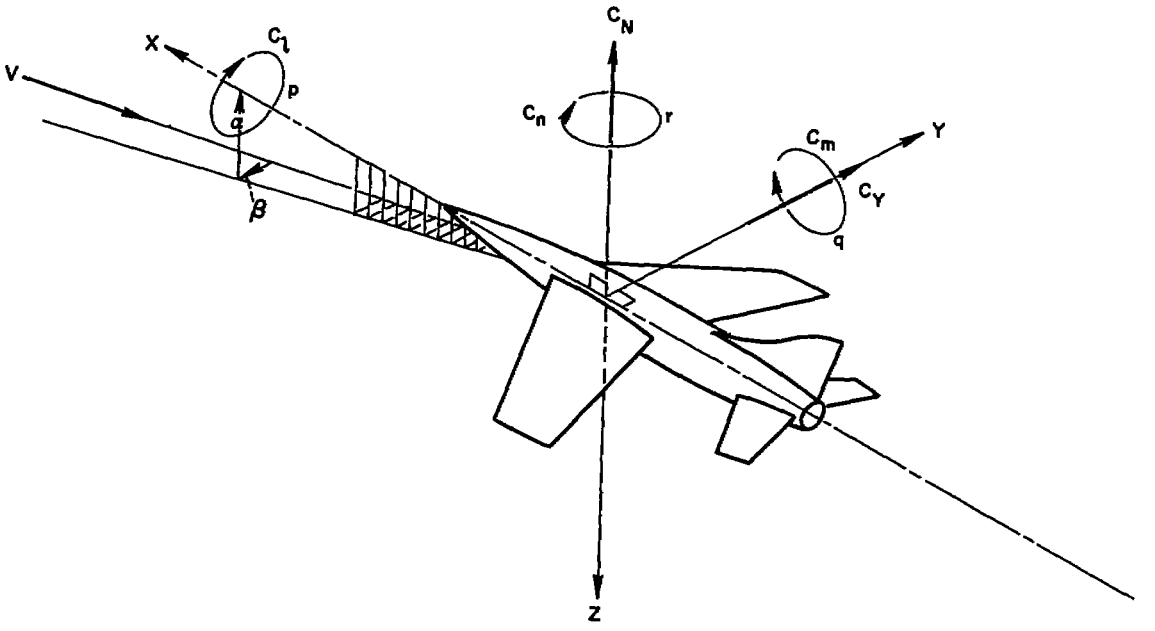

Figure 2.- System of axes with positive direction of forces, moments, and angles indicated by arrows.

[redacted]

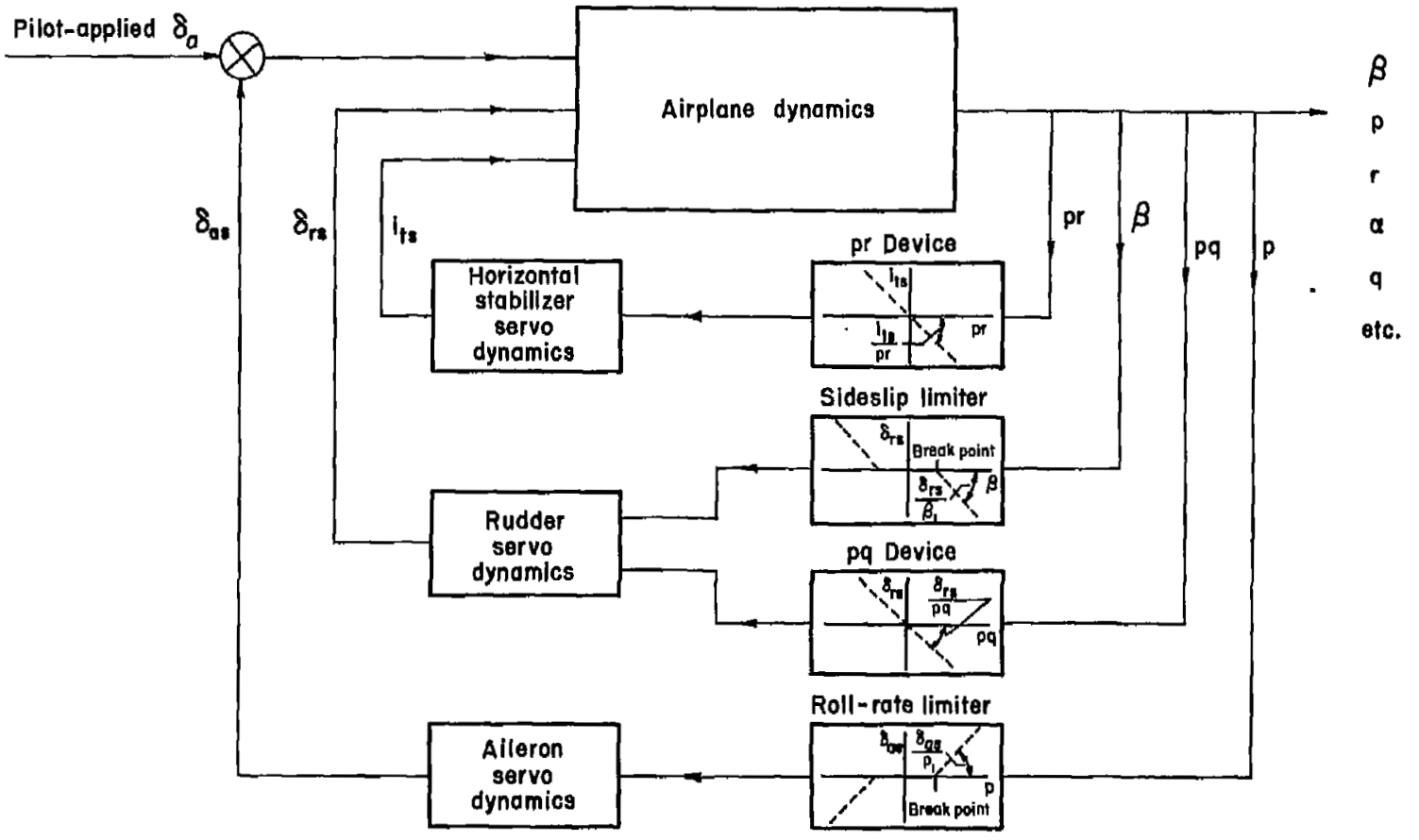

Figure 3.- Simplified block diagram of stability augmentation systems.

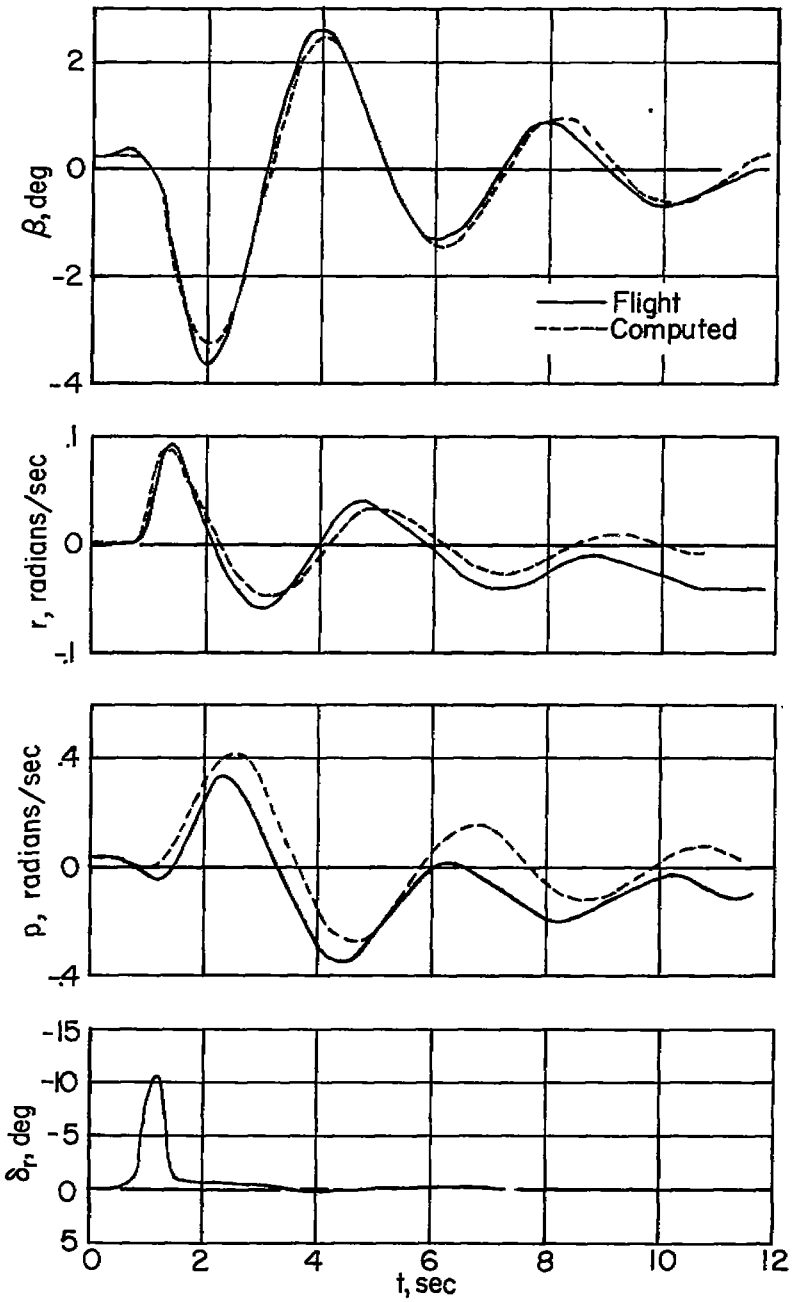

(a) Rudder pulse at M=0.71, h_p=30,700.

Figure 4.- Comparison of airplane response with analog-computed response.

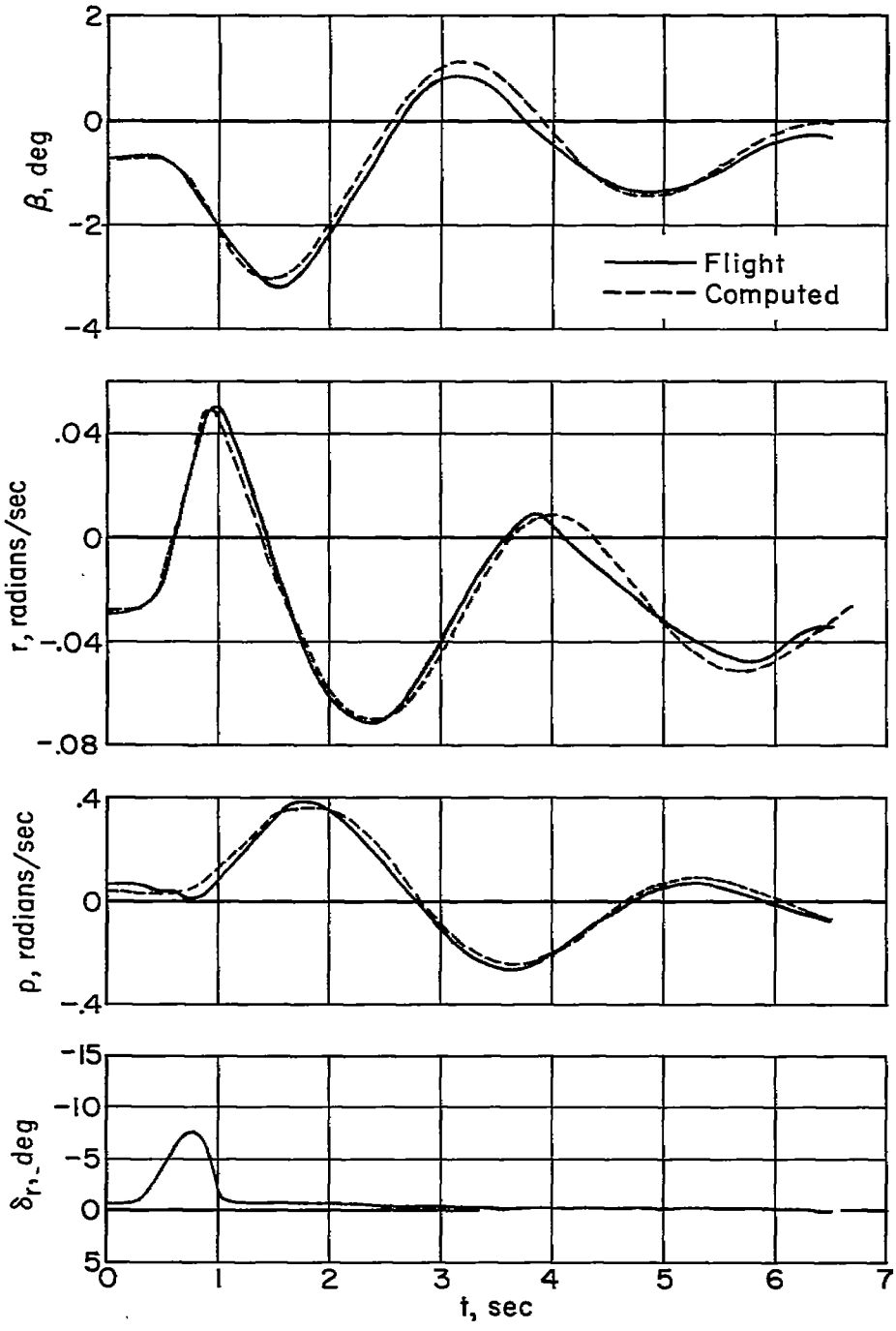

(b) Rudder pulse at M = 0.90, h_p = 40,000.

Figure 4.- Continued.

[redacted]

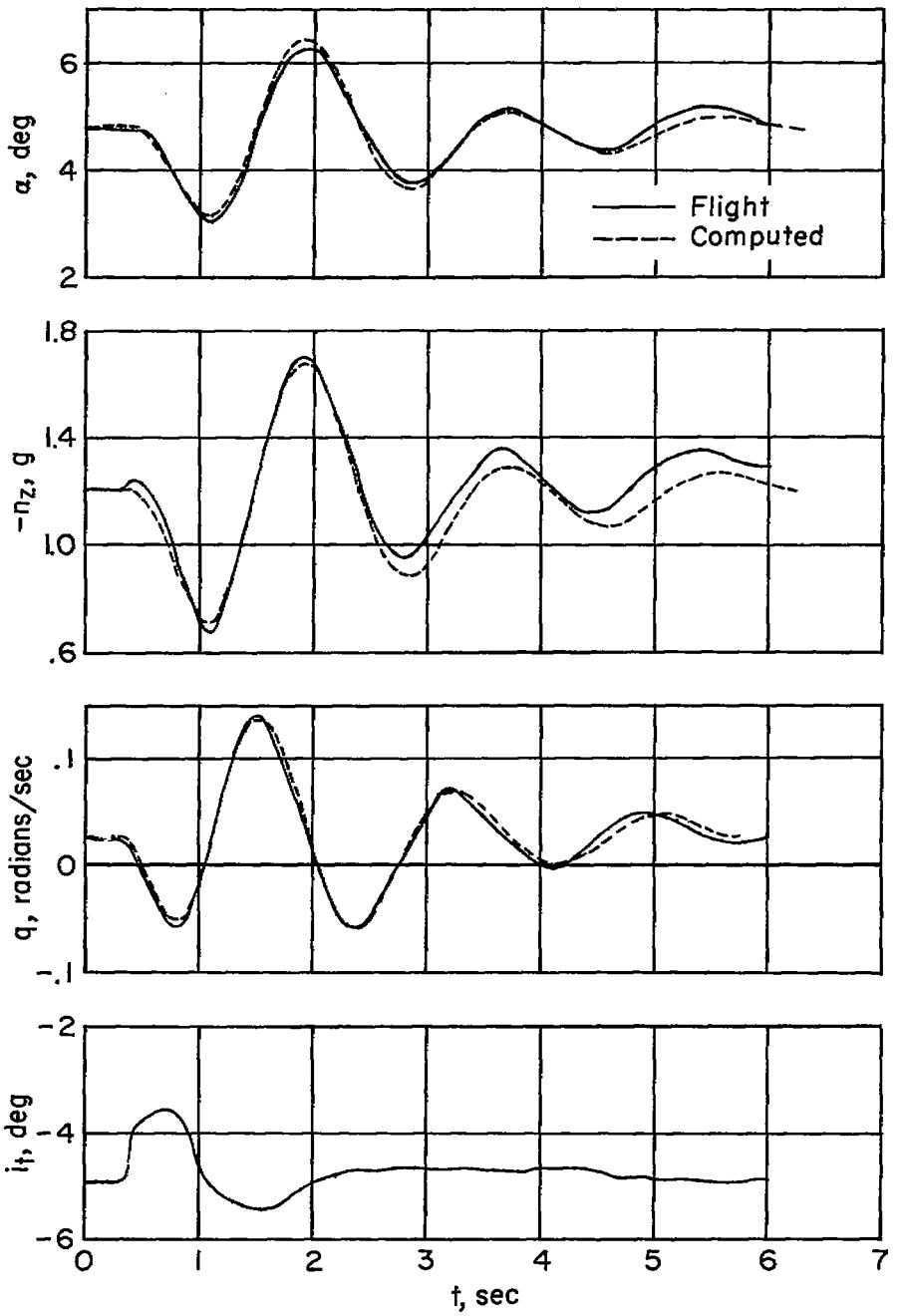

(c) Stabilizer pulse at M=0.90, h_p= 40,000.

Figure 4.- Concluded.

[redacted]

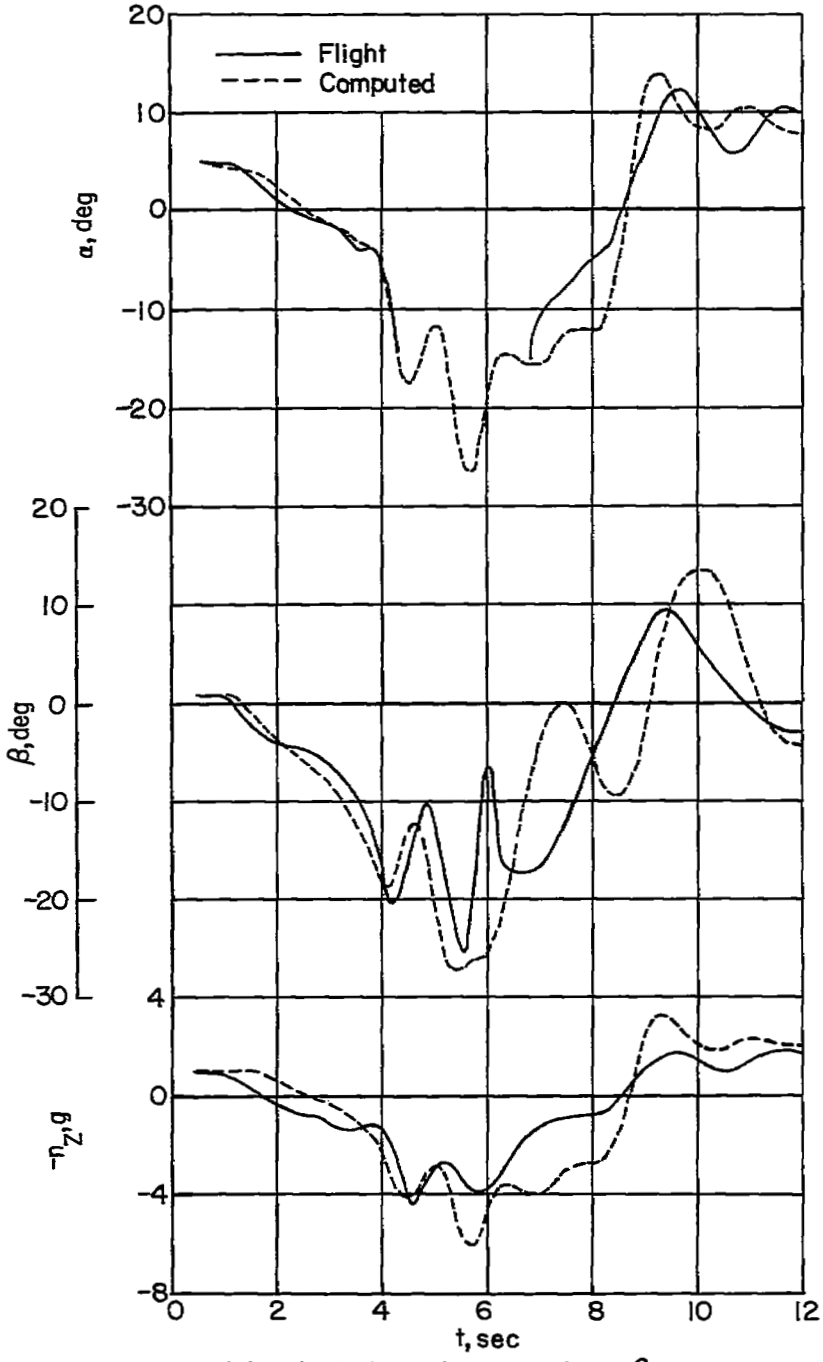

(a) Flight time histories of α, β and n_z.

Figure 5.- Comparison of flight time history of reference 1 with analog-computed time history; M = 0.70, $h_p \approx 30{,}000$.

[redacted]

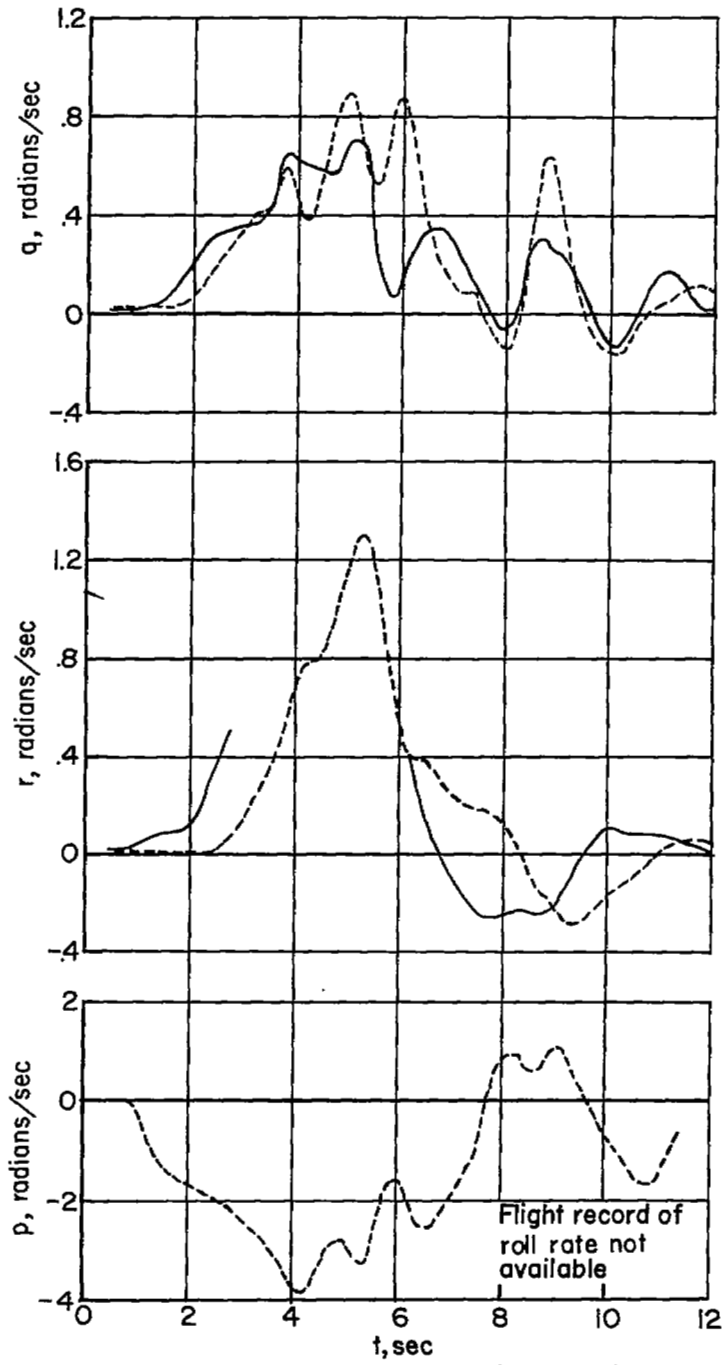

(b) Flight time histories of q, r and p.

Figure 5.- Concluded.

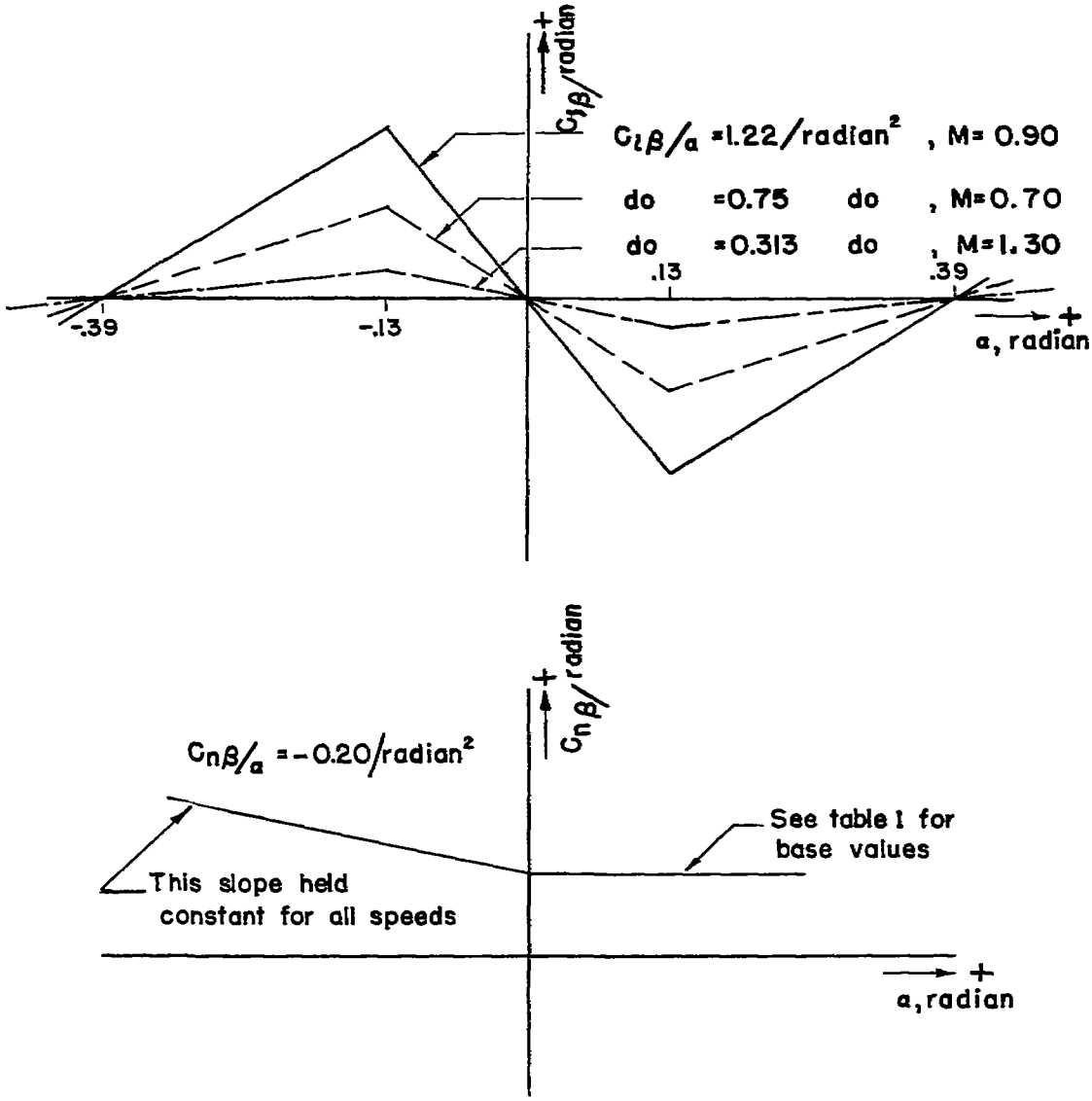

Figure 6.- Illustration of nonlinear stability derivatives used in F-100 roll-coupling study.

[redacted]

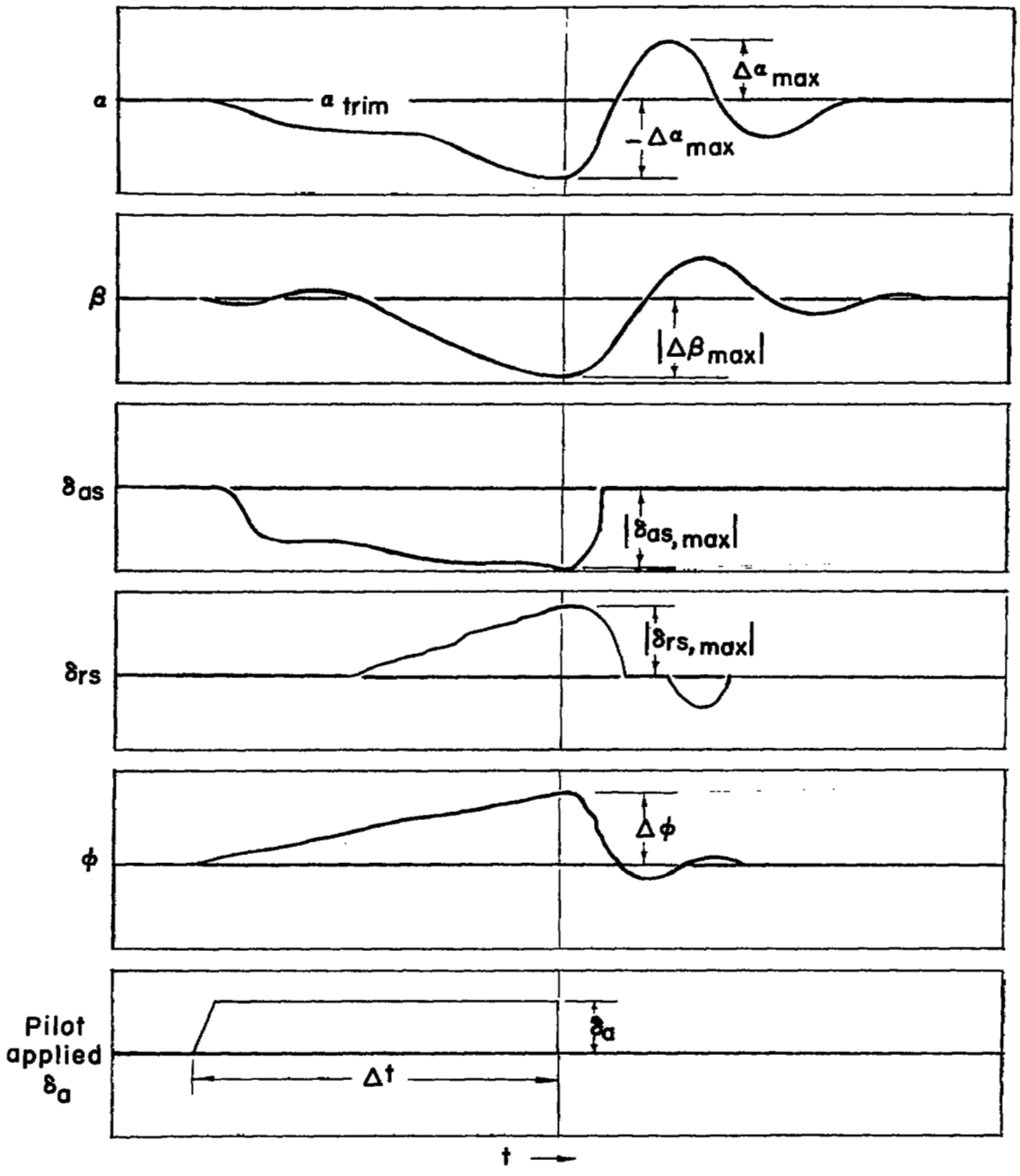

Figure 7.- Typical computed time history illustrating quantities used in plotting results of stability augmentation study.

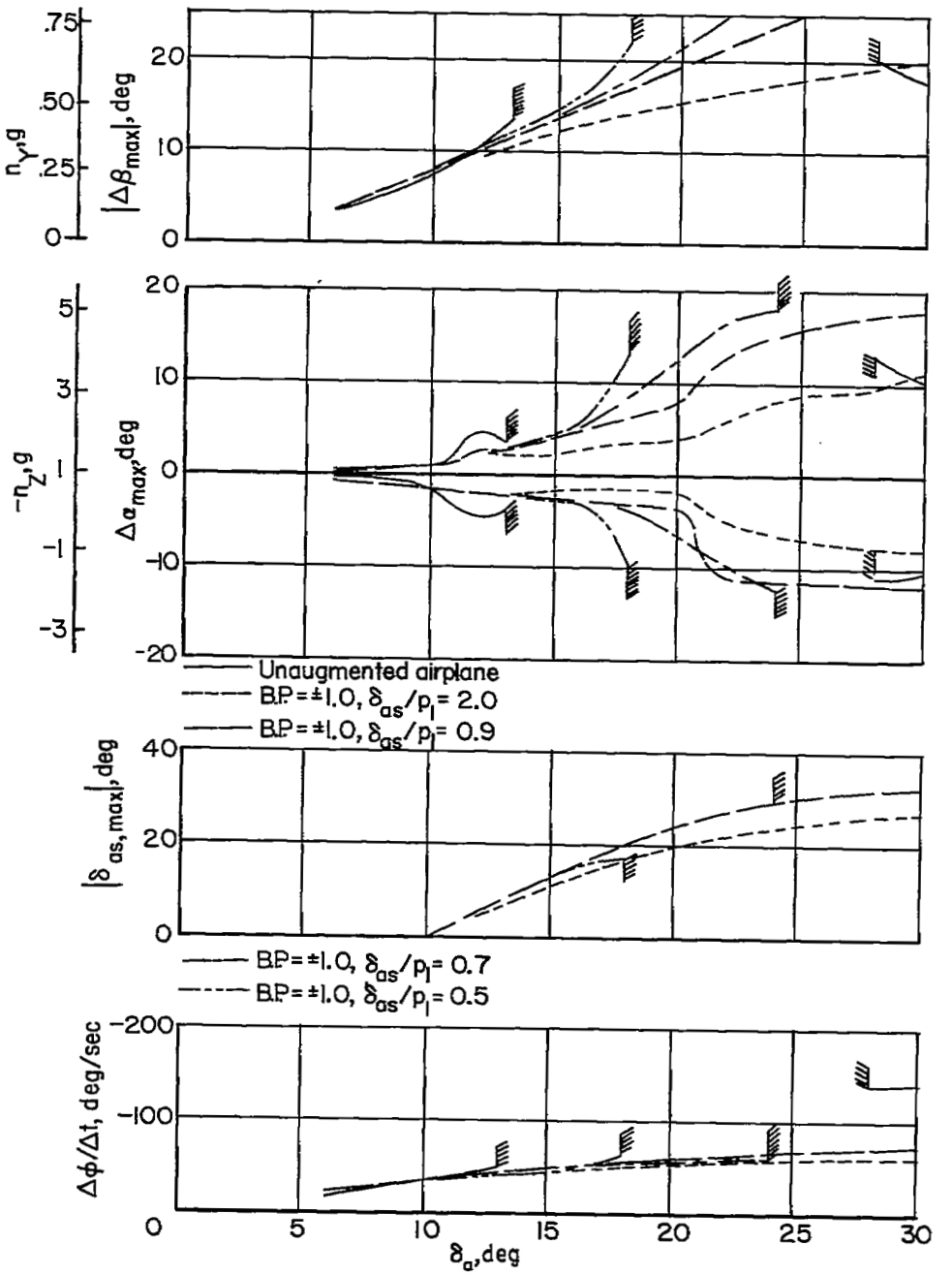

Figure 8.- Effect of roll-rate limiter gearing δ_{as}/p_1 on the airplane motion during a 360° rolling maneuver initiated from 1g wings-level flight at M = 0.70, h_p = 32,000.

[redacted]

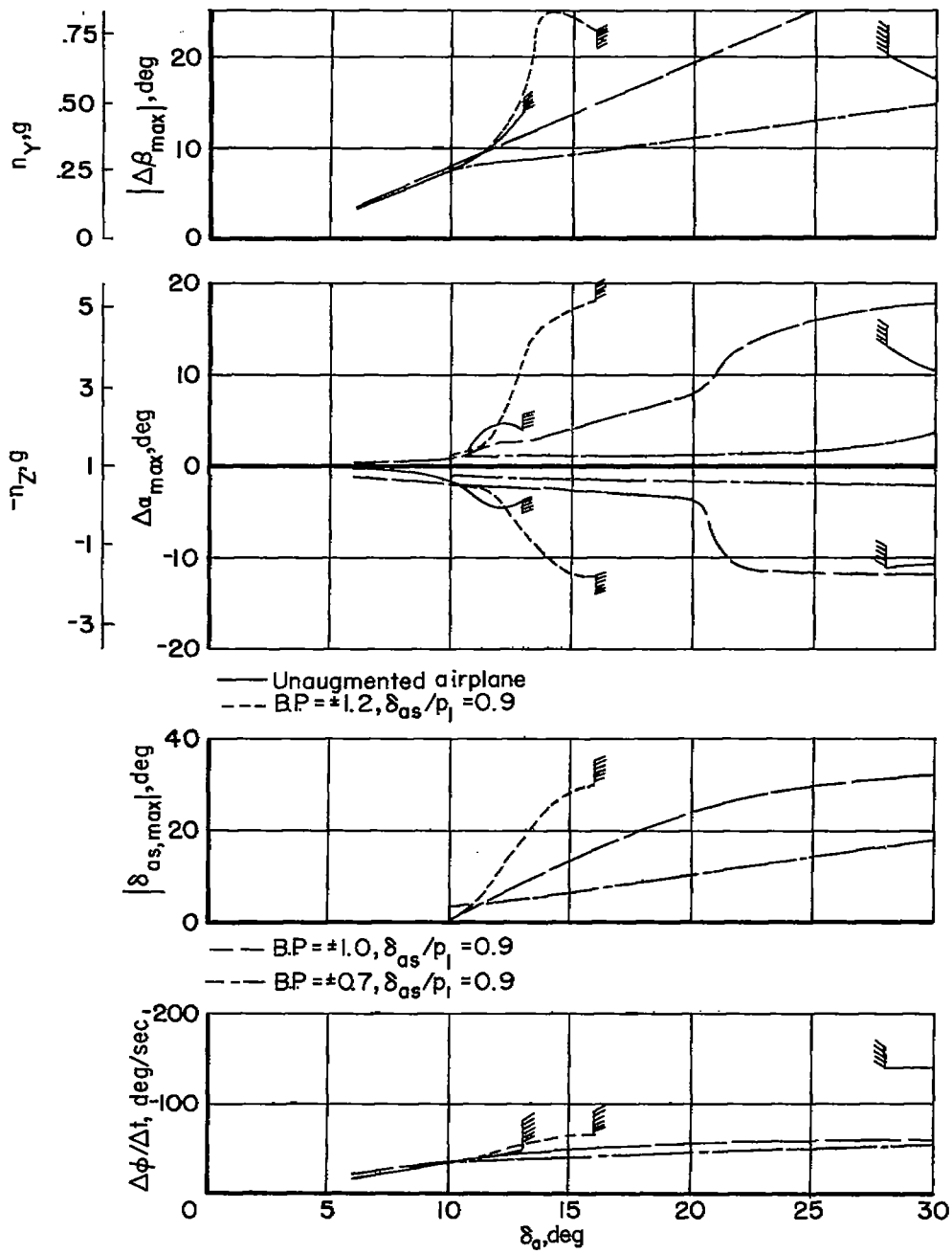

Figure 9.- Effect of roll-rate limiter break point on the airplane motion during a 360° rolling maneuver initiated from 1g wings-level flight at M = 0.70, h_p = 32,000.

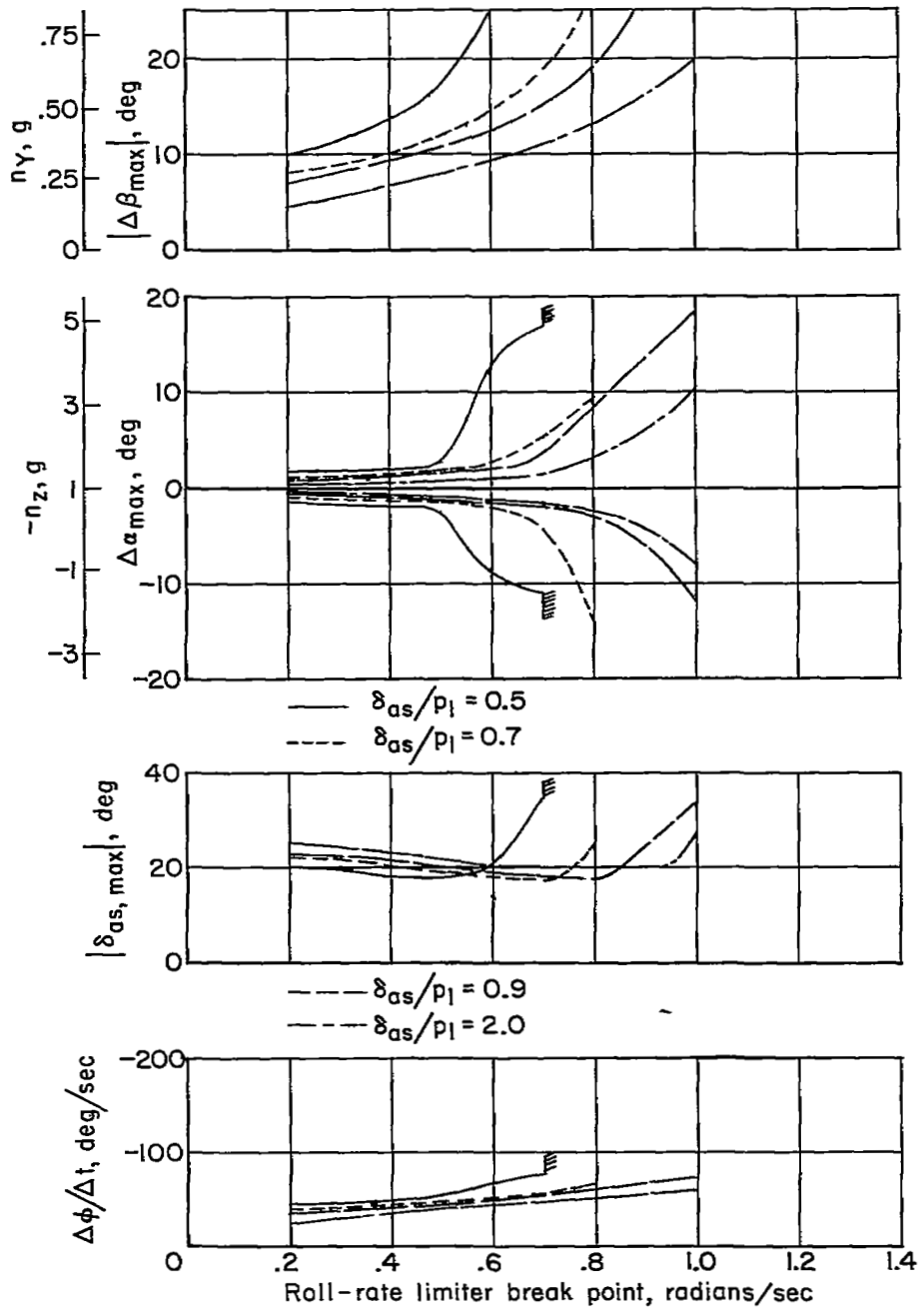

Figure 10.- Cross plot showing effect of roll-rate limiter break point and gearing on the airplane motions during a 360° rolling maneuver initiated from 1g wings-level flight using a constant input disturbance of 30° aileron deflection; M = 0.70, h_p = 32,000.

[redacted]

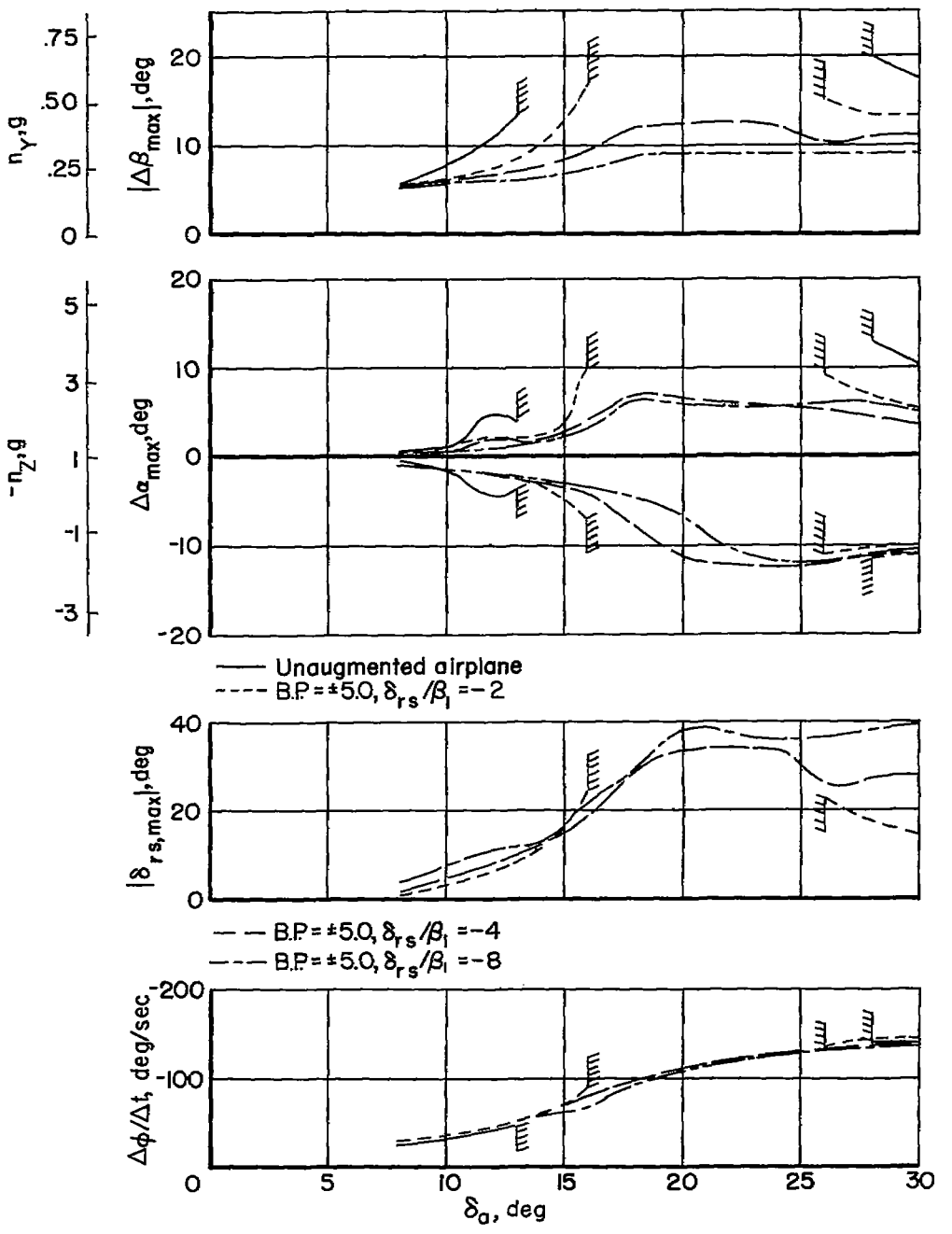

Figure 11.- Effect of sideslip limiter gearing on the airplane motion during a 360° rolling maneuver initiated from 1g wings-level flight at M = 0.70, h_p = 32,000.

[redacted]

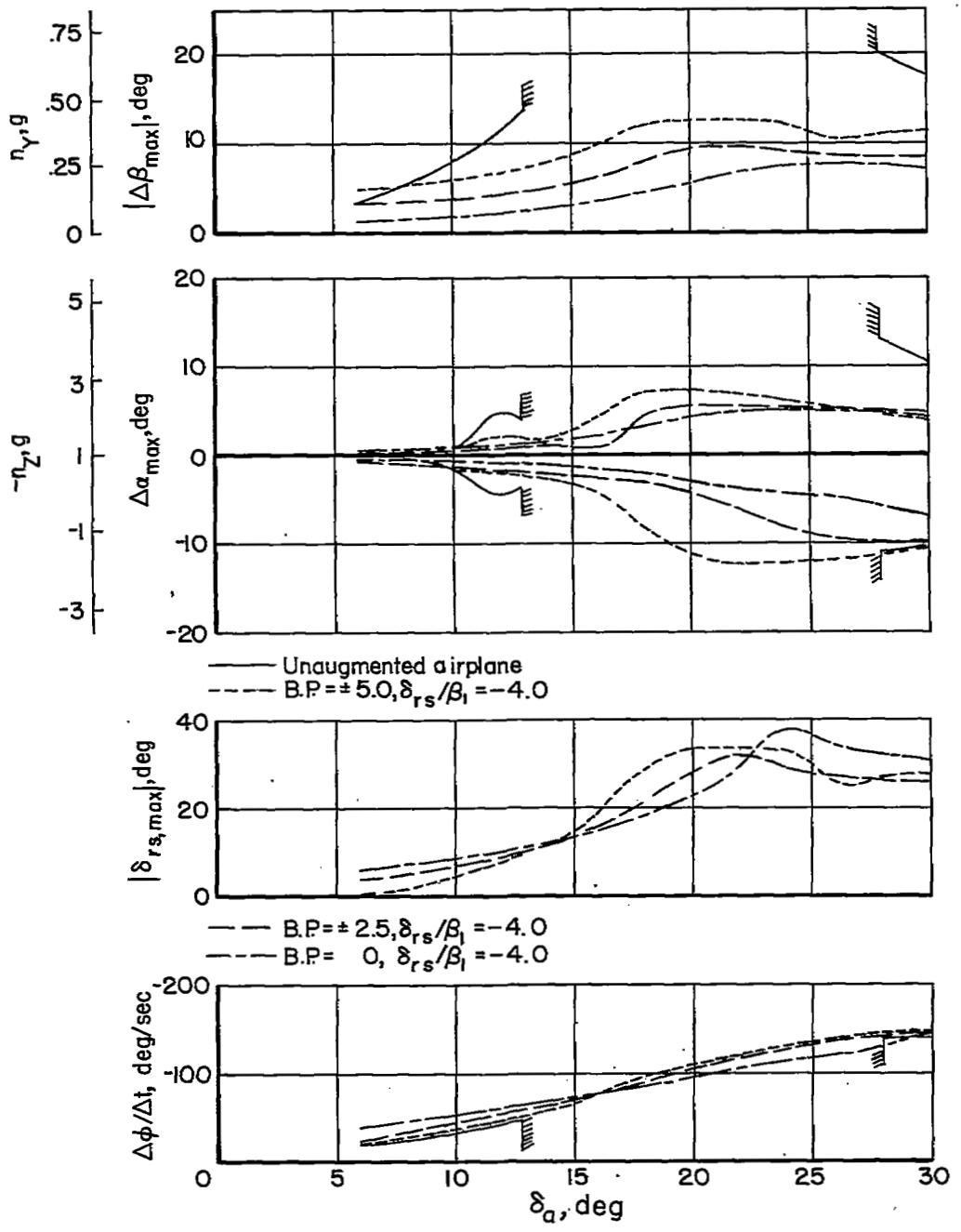

Figure 12.- Effect of sideslip limiter break point on the airplane motion during a 360° rolling maneuver initiated from 1g wings-level flight at M = 0.70, h_p = 32,000.

[redacted]

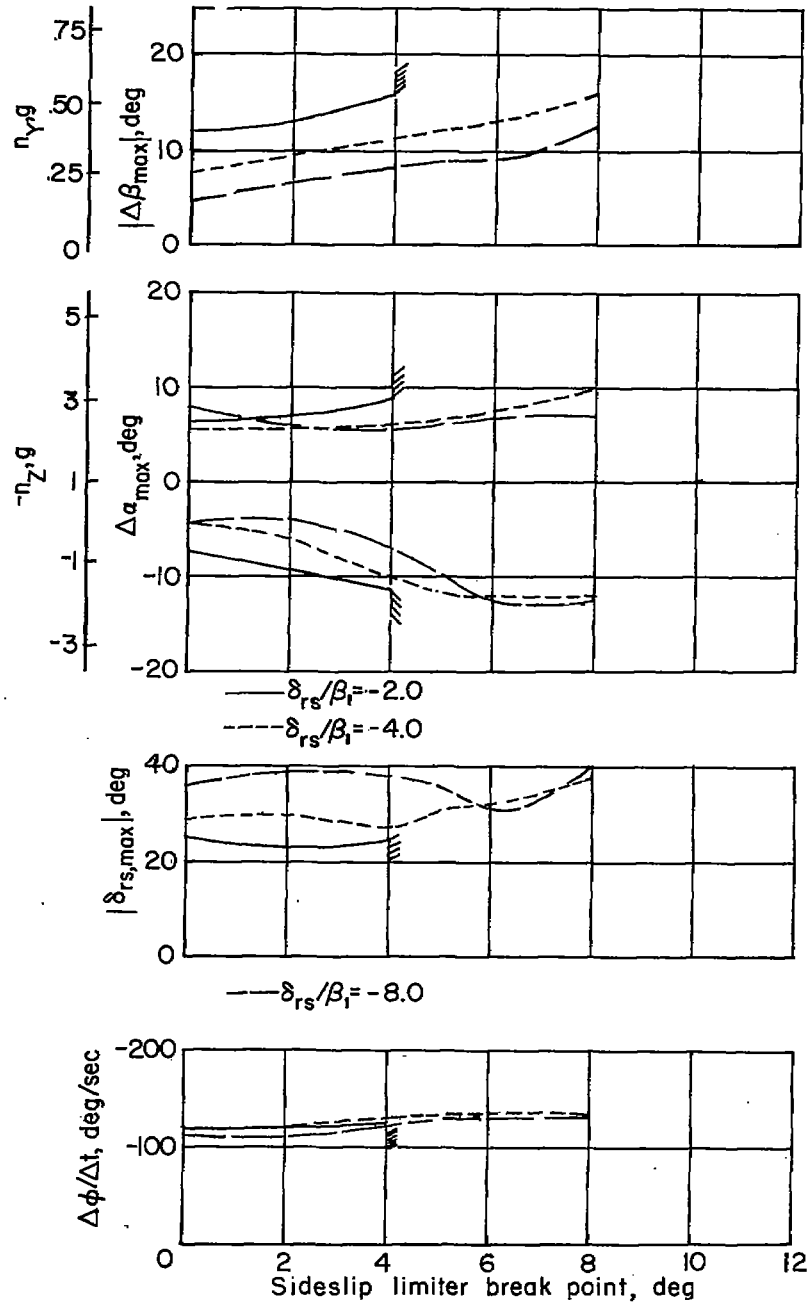

Figure 13.- Cross plot showing effect of sideslip limiter break point and gearing on the airplane motion during a 360° rolling maneuver initiated from 1g wings-level flight using a constant input disturbance of 22° aileron deflection at M = 0.70, h_p = 32,000.

[redacted]

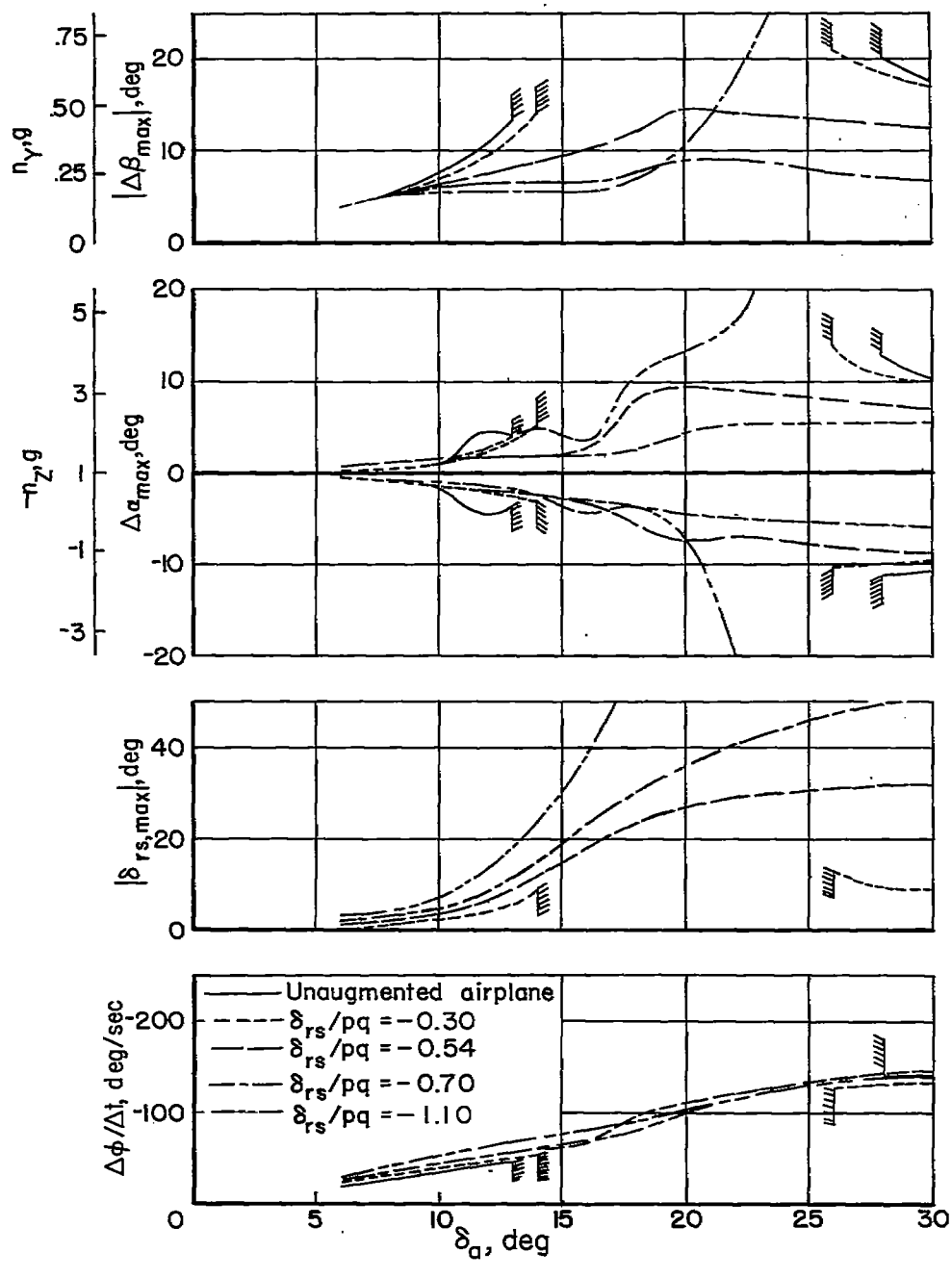

Figure 14.- Effect of δ_{rs}/pq gearing on the airplane motion during a 360° roll maneuver initiated from 1g wings-level flight at M = 0.70, h_p = 32,000.

[redacted]

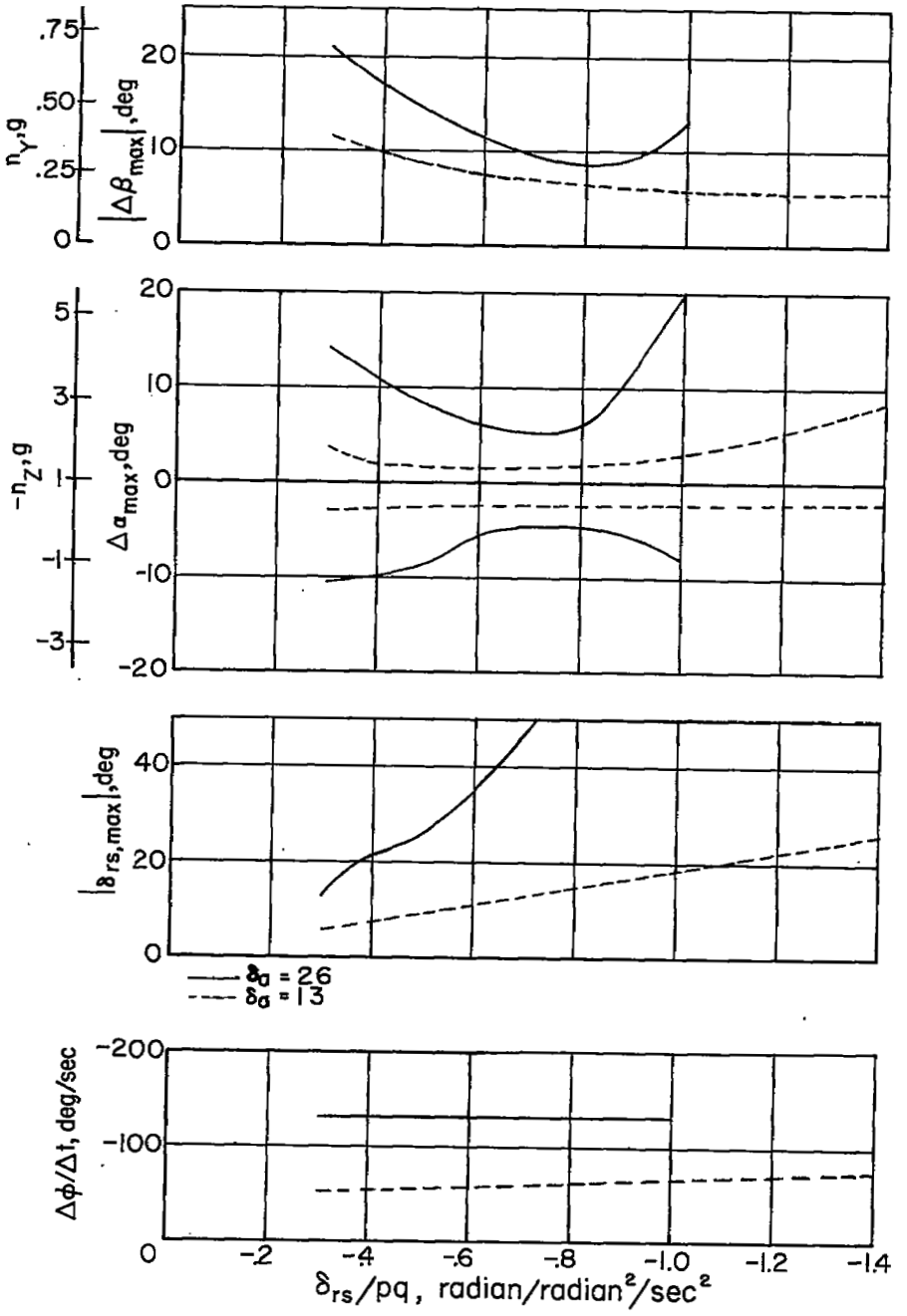

Figure 15.- Cross plot showing effect of δ_{rs}/pq gearing on the airplane motions during a 360° rolling maneuver initiated from 1g wings-level flight using constant input disturbance of 26° and 13° aileron deflection; M = 0.70, h_p = 32,000.

[redacted]

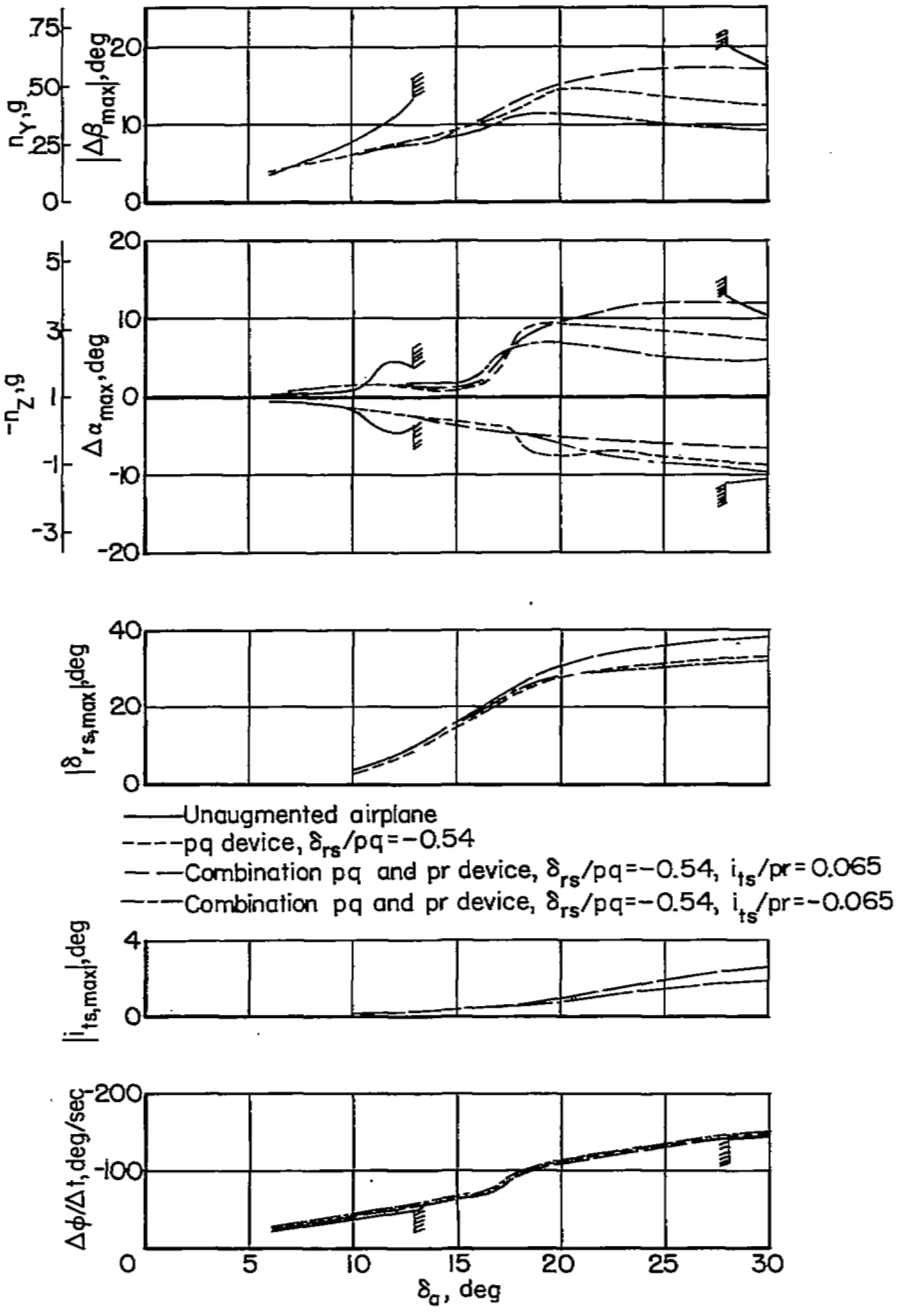

Figure 16.- Comparison of stability augmentation system employing pq feedback alone with stability augmentation system employing both pq and pr feedback on the airplane motions during a 360° rolling maneuver initiated from 1g wings-level flight at M = 0.70, h_p = 32,000.

[redacted]

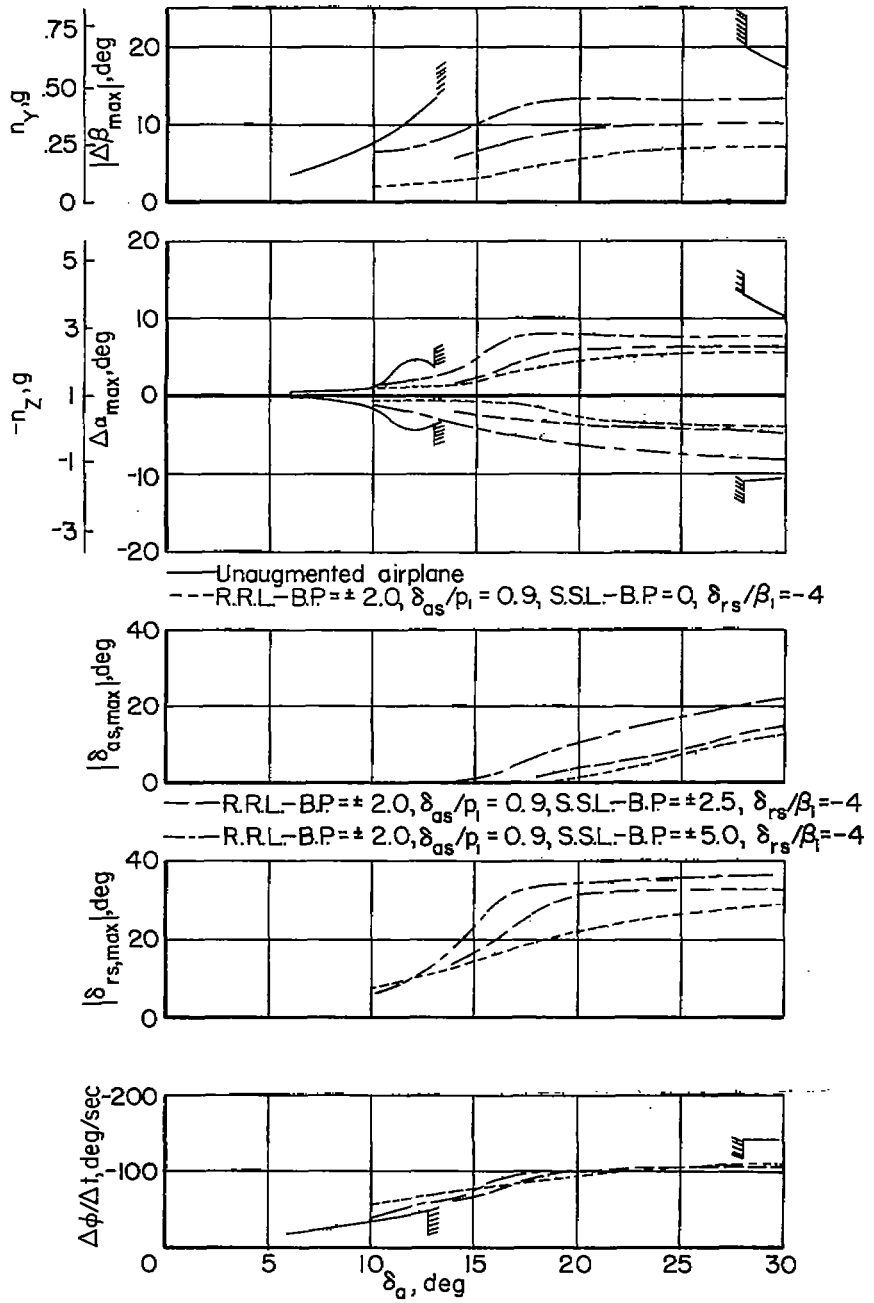

Figure 17.- Effect of sideslip limiter break point on the airplane motions during a 360° rolling maneuver initiated from 1g wings-level flight of an airplane augmented by a combination roll-rate limiter and sideslip limiter at M = 0.70, h_p = 32,000.

[redacted]

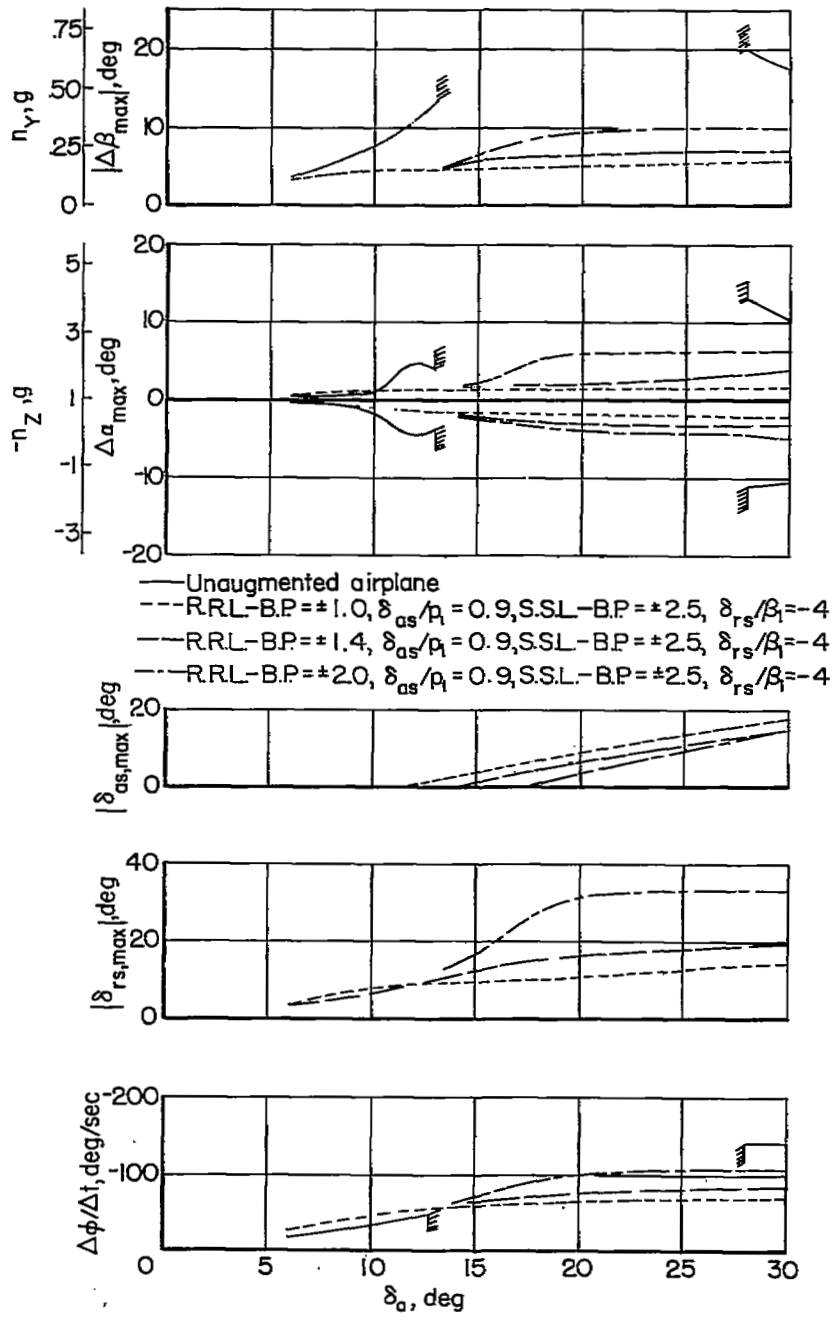

Figure 18.- Effect of roll-rate limiter break point on the airplane motions during a 360° rolling maneuver initiated from 1g wings-level flight of an airplane augmented by a combination roll-rate limiter and sideslip limiter at M = 0.70, h_p = 32,000.

[redacted]

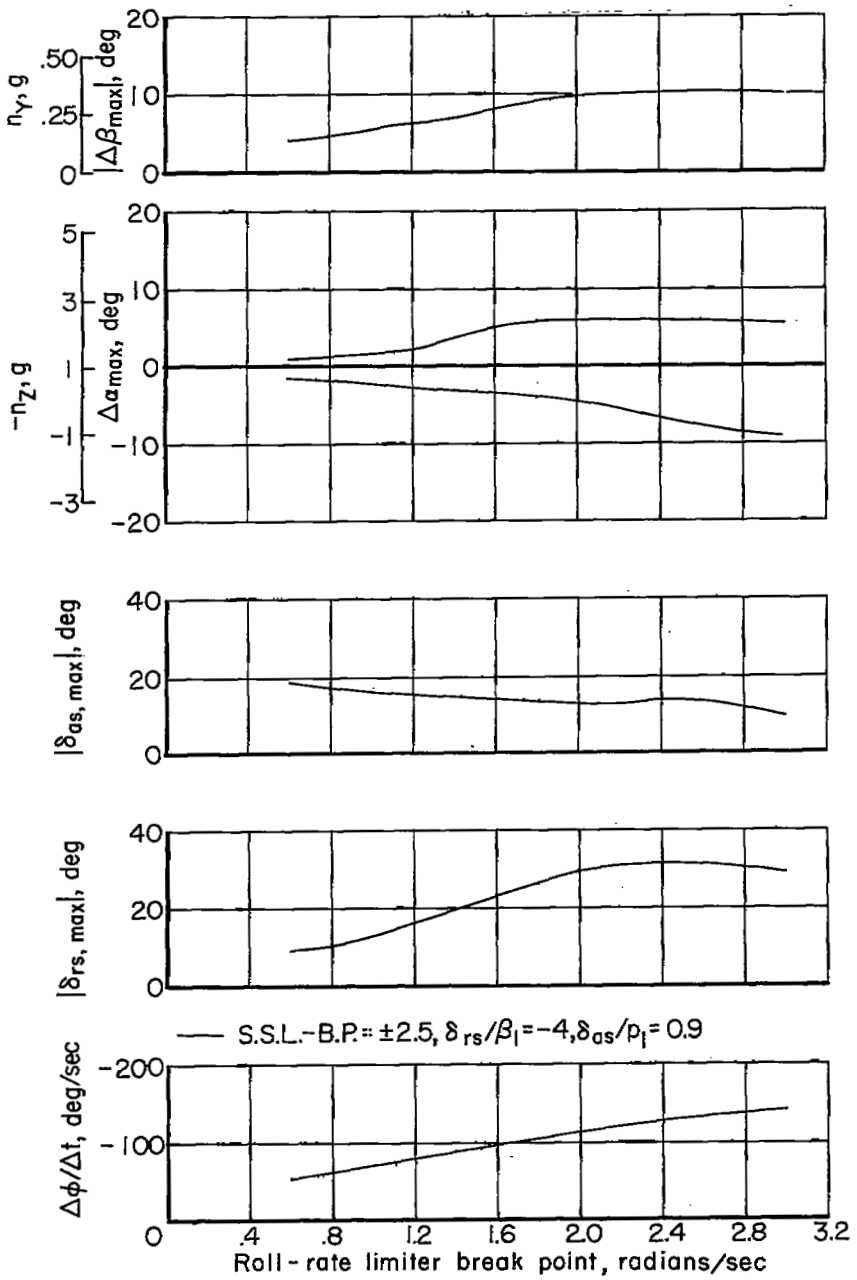

Figure 19.- Cross plot at constant input disturbance of $\delta_a = 30^\circ$, showing effect of roll-rate limiter break point on the airplane motions during a 360° rolling maneuver initiated from 1g wings-level flight of an airplane augmented by a combination roll-rate limiter and sideslip limiter at $M = 0.70$, $h_p = 32{,}000$.

[redacted]

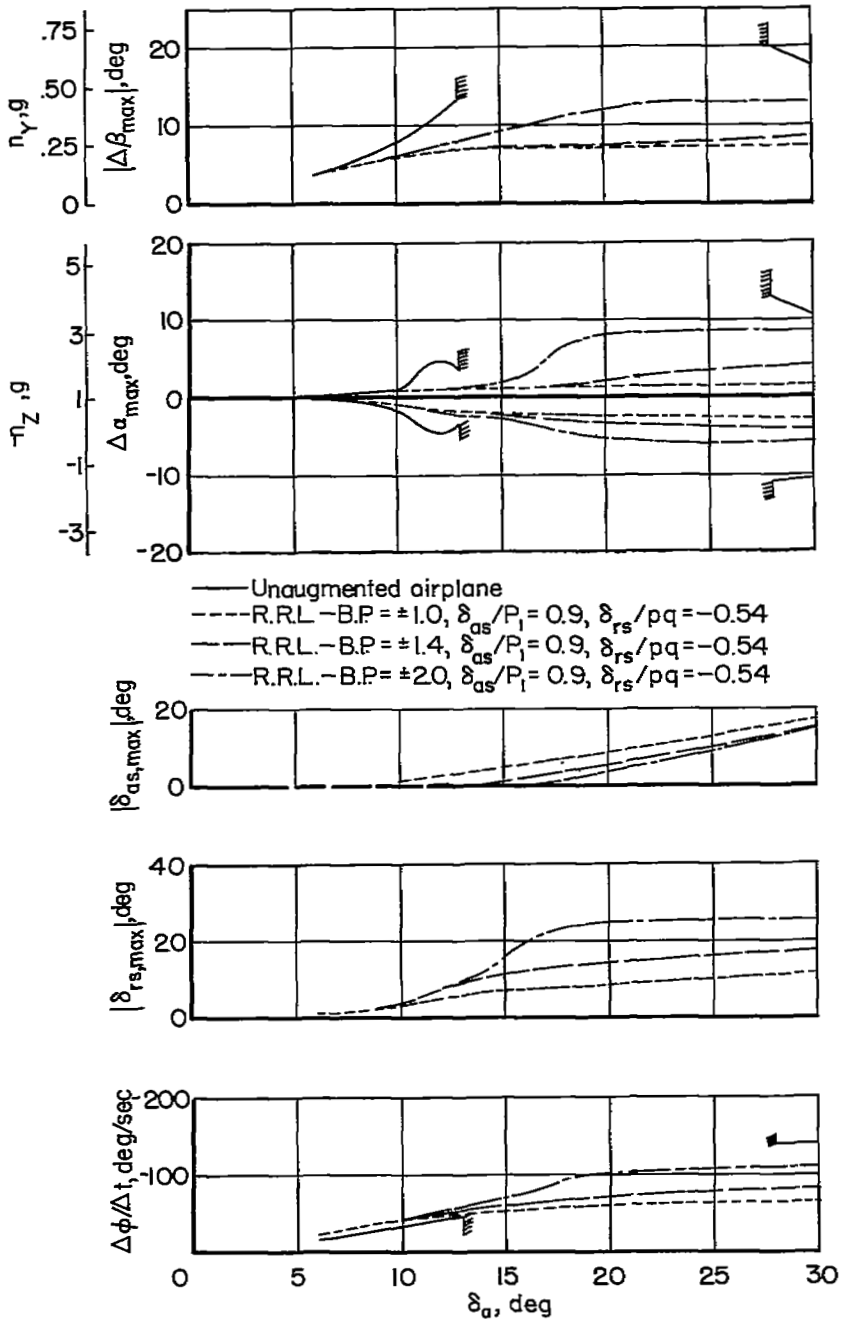

Figure 20.- Effect of roll-rate limiter break point on the airplane motions during a 360° rolling maneuver initiated from 1g wings-level flight of an airplane augmented by a combination roll-rate limiter and pq device at M = 0.70, h_p = 32,000.

[redacted]

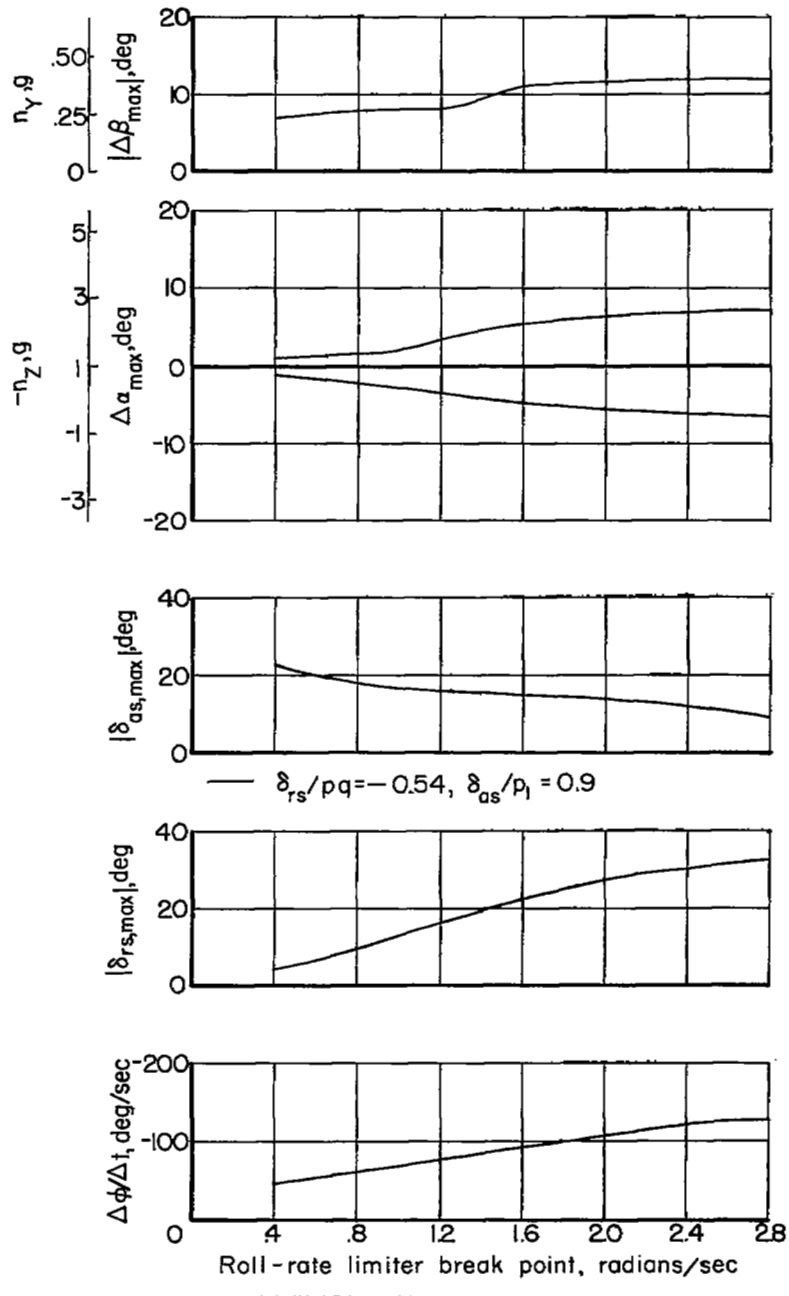

Figure 21.- Cross plot at constant input disturbance of $\delta_a = 30^\circ$, showing effect of roll-rate limiter break point on the airplane motions during a 360° rolling maneuver initiated from 1g wings-level flight of an airplane augmented by a combination roll-rate limiter and pq device at M = 0.70, h_p = 32,000.

[redacted]

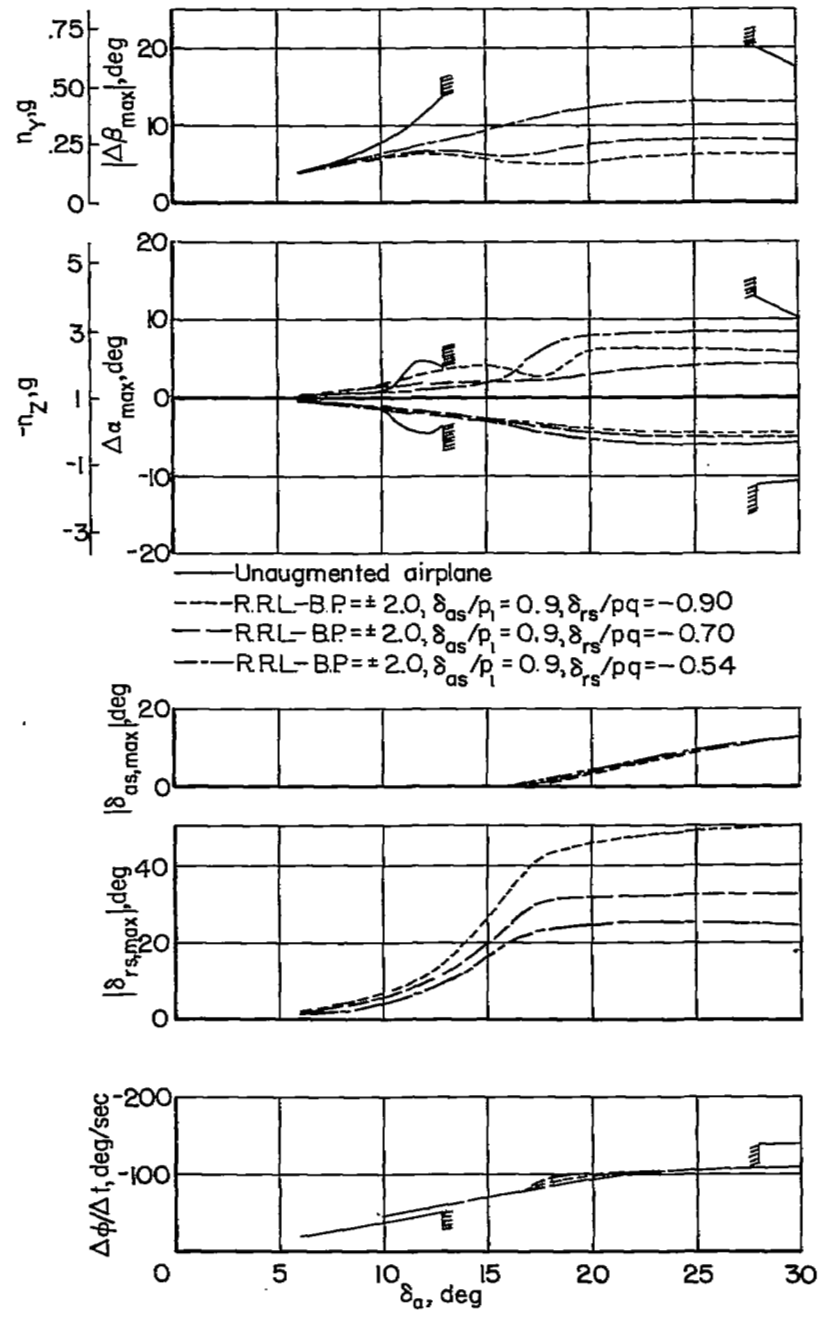

Figure 22.- Effect of δ_{rs}/pq gearing on the airplane motions during a 360° rolling maneuver initiated from 1g wings-level flight of an airplane augmented by a combination roll-rate limiter and pq device at M = 0.70, h_p = 32,000.

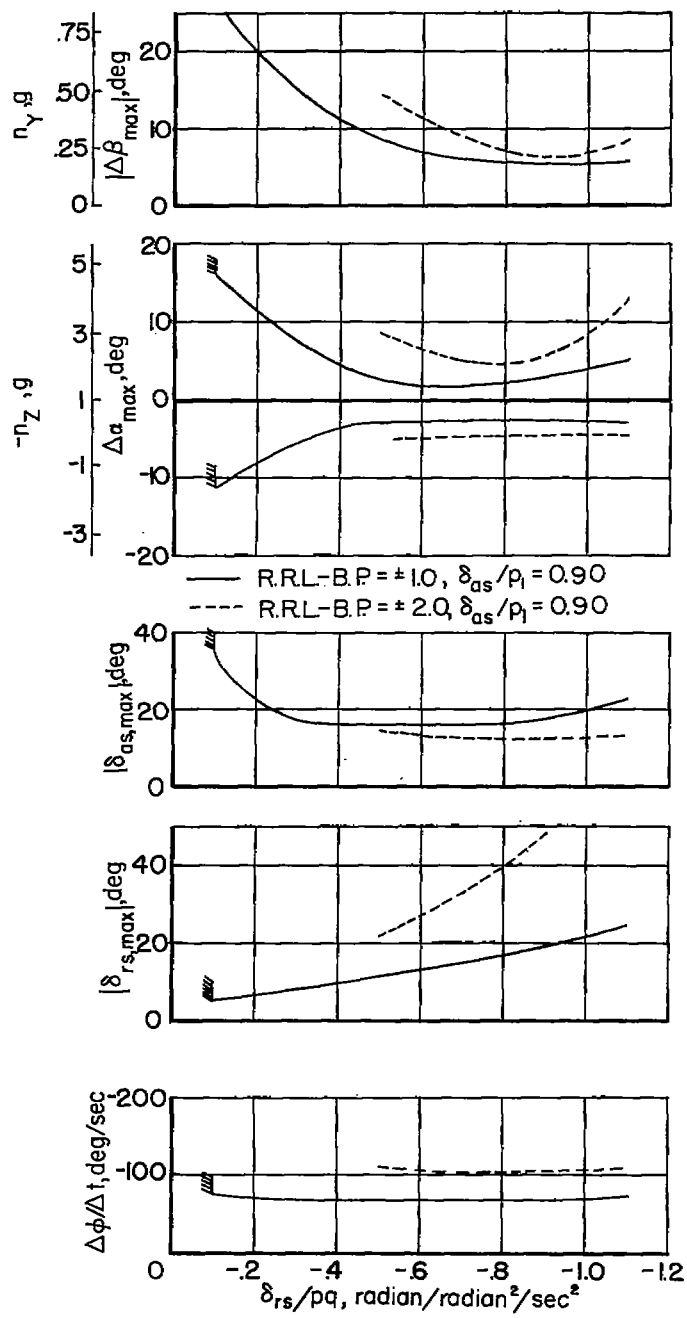

Figure 23.- Cross plot at constant input disturbance of $\delta_a = 30^\circ$, showing effect of δ_{rs}/pq gearing on the airplane motions during a 360° rolling maneuver initiated from 1g wings-level flight of an airplane augmented by a combination roll-rate limiter and pq device at M = 0.70, h_p = 32,000.

[redacted]

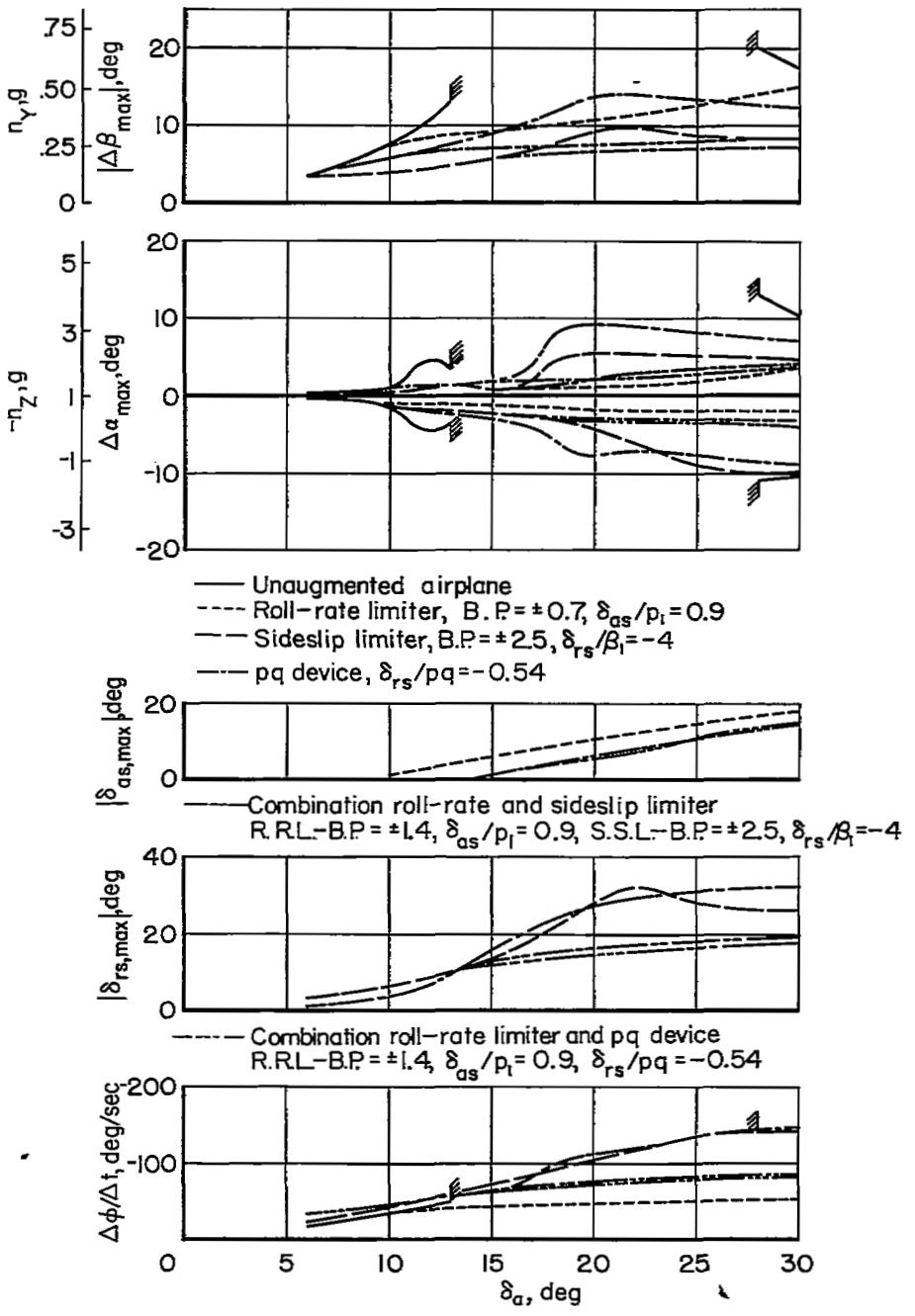

Figure 24.- Summary plot showing the effect of various stability augmentation schemes on the airplane motion during a 360° rolling maneuver initiated from 1g wings-level flight at M = 0.70, h_p = 32,000.

[redacted]

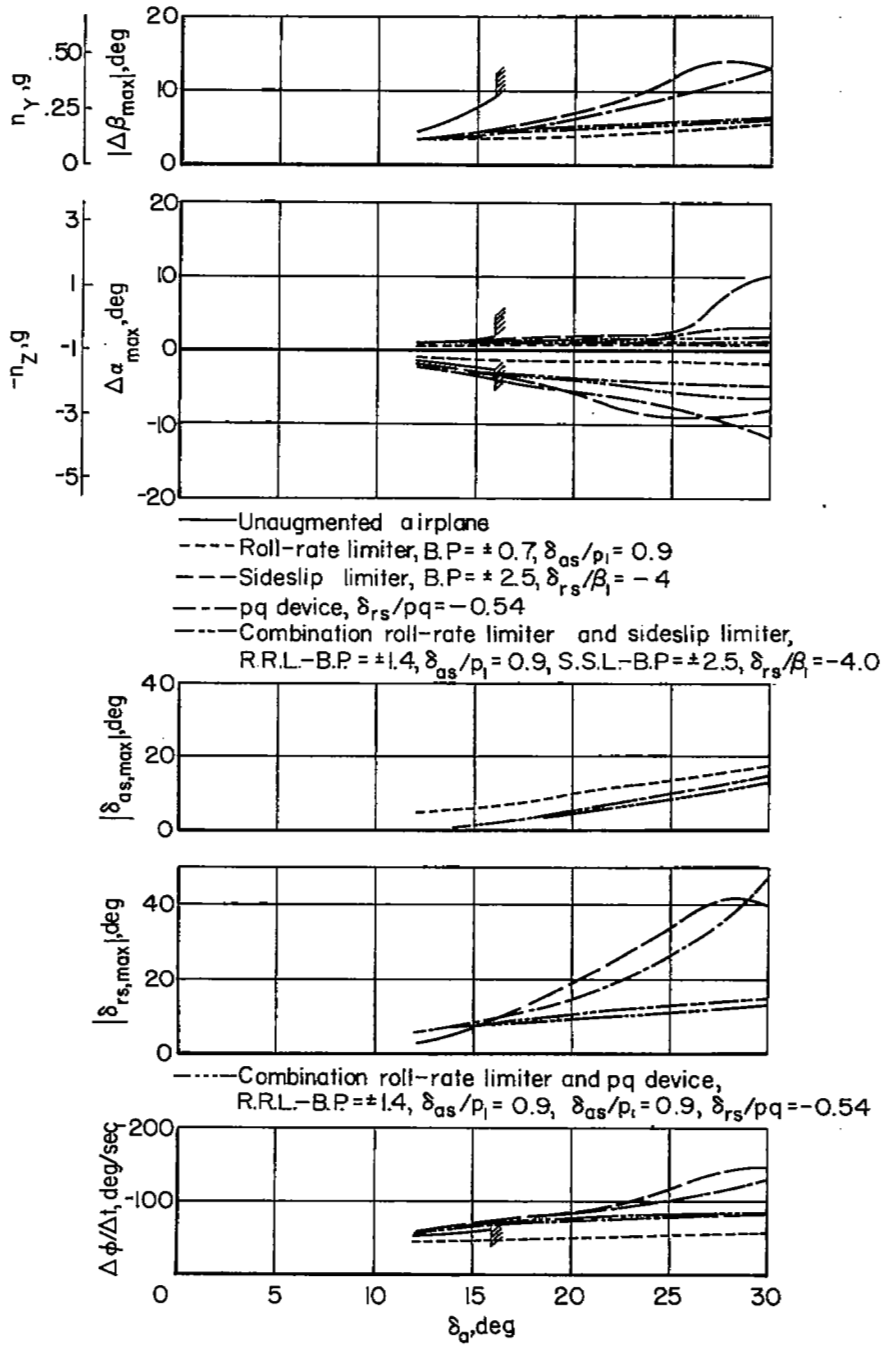

Figure 25.- Summary plot showing the effect of various stability augmentation schemes on the airplane motion during a 360° rolling maneuver initiated from -1g wings-level flight at M = 0.70, h_p = 32,000.

[redacted]

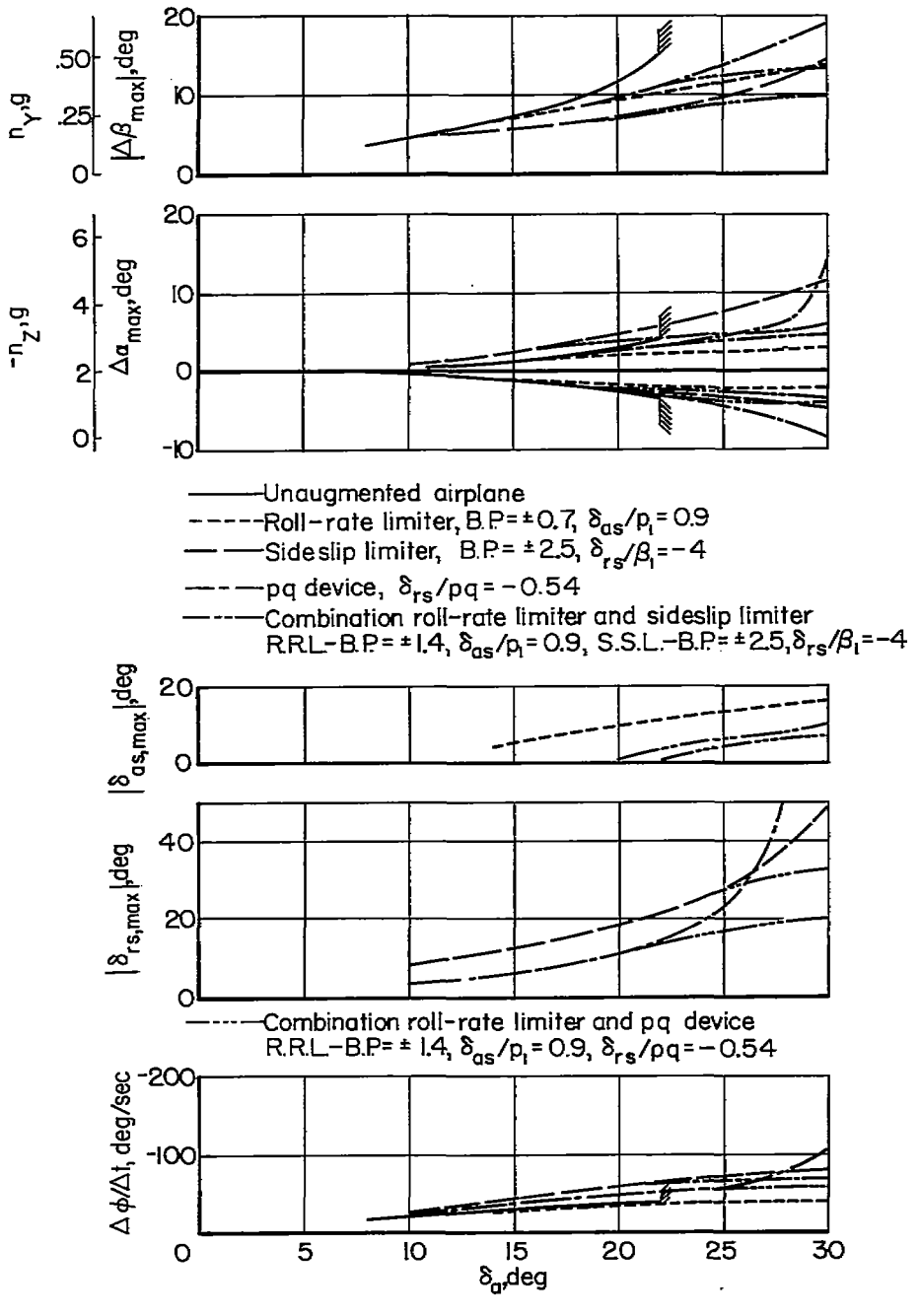

Figure 26.- Summary plot showing the effect of various stability augmentation schemes on the airplane motion during a 360° rolling maneuver initiated from a 2g coordinated turn at M = 0.70, h_p = 32,000.

[redacted]

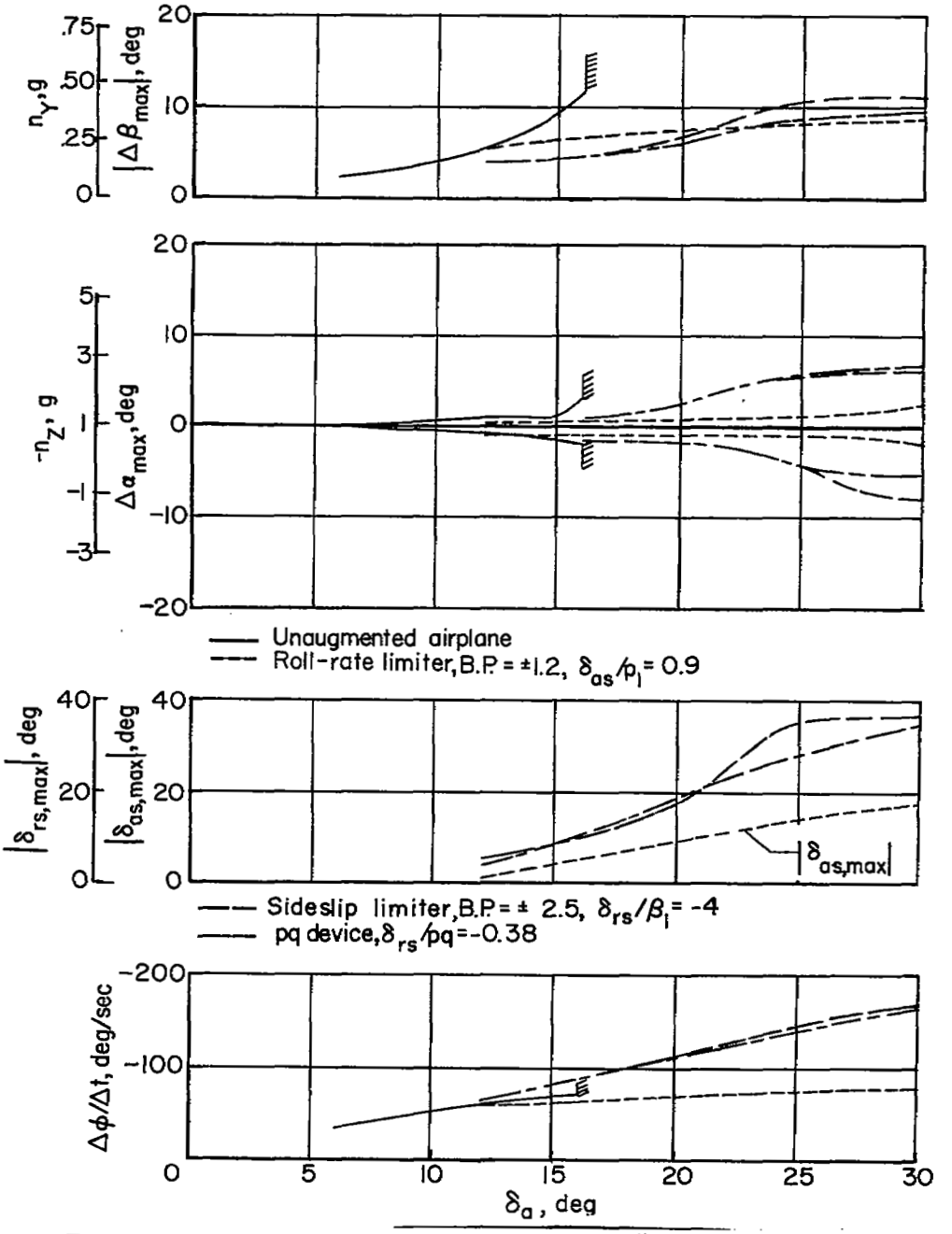

Figure 27.- Summary plot showing the effect of various stability augmentation schemes on the airplane motion during a 360° rolling maneuver initiated from 1g wings-level flight at M = 0.90, h_p = 40,000.

[redacted]

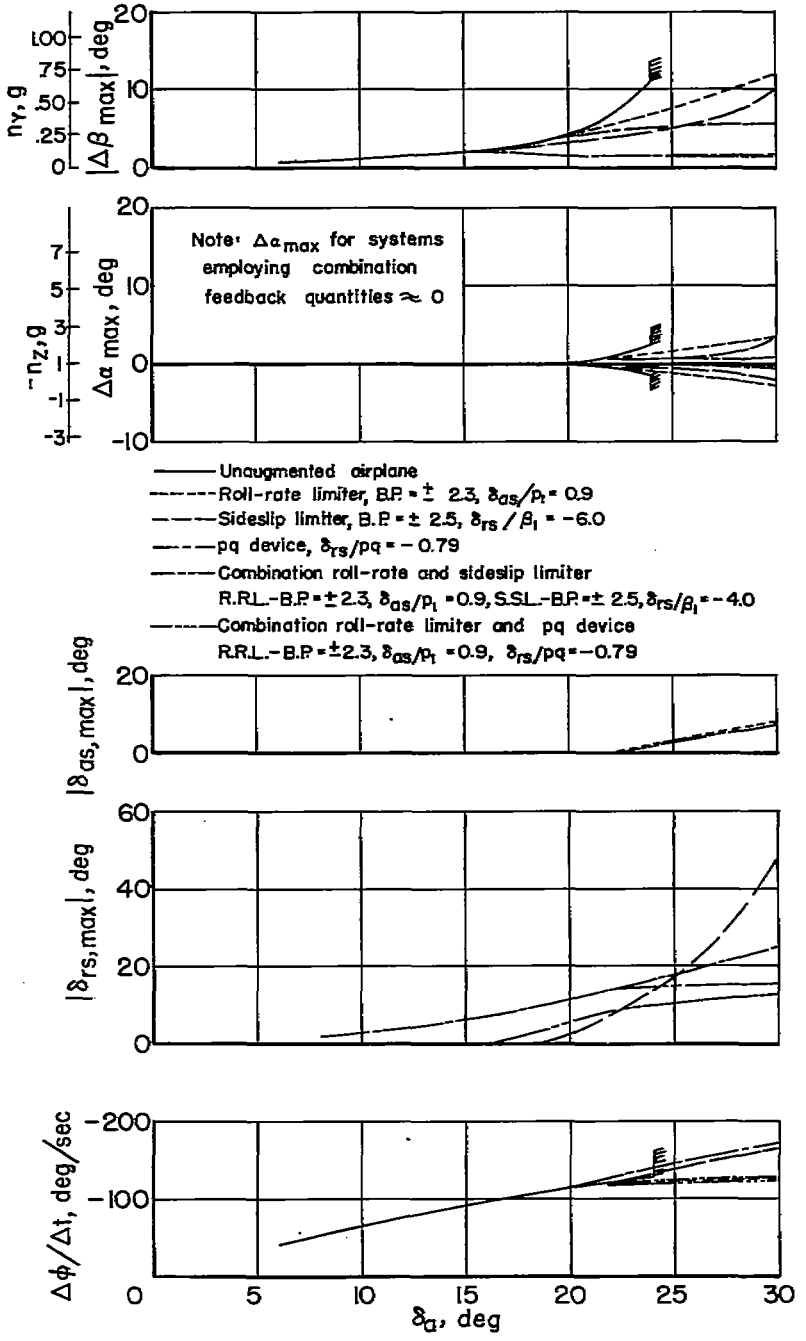

Figure 28.- Summary plot showing the effect of various stability augmentation schemes on the airplane motions during a 720° rolling maneuver initiated from 1g wings-level flight at M = 1.3, h_p = 40,000.

[redacted]

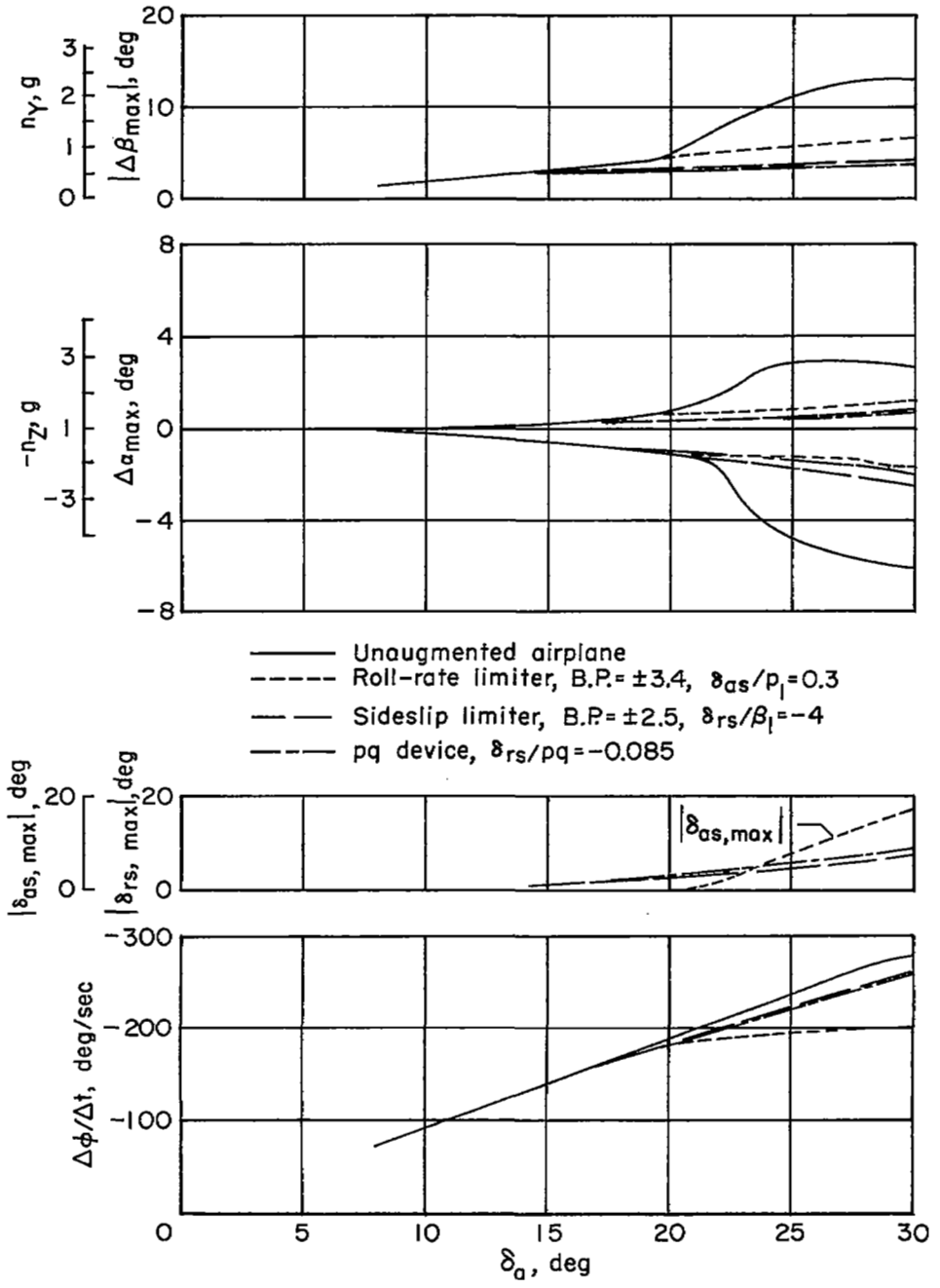

Figure 29.- Summary plot showing the effect of various stability augmentation schemes on the airplane motions during a 720° rolling maneuver initiated from 1g wings-level flight at M = 0.90, h_p = 5,000.